Since January 2020 Elsevier has created a COVID-19 resource centre with free information in English and Mandarin on the novel coronavirus COVID-19. The COVID-19 resource centre is hosted on Elsevier Connect, the company's public news and information website.

Chaos, Solitons and Fractals 135 (2020) 109867

Contents lists available at ScienceDirect

Chaos, Solitons and Fractals

Nonlinear Science, and Nonequilibrium and Complex Phenomena

journal homepage: www.elsevier.com/locate/chaos

On a comprehensive model of the novel coronavirus (COVID-19) under Mittag-Leffler derivative

Mohammed S. Abdo[a,b,*], Kamal Shah[c], Hanan A. Wahash[a], Satish K. Panchal[a]

[a] Department of Mathematics, Dr. Babasaheb Ambedkar Marathwada University, Aurangabad, (M.S), 431001, India
[b] Department of Mathematics, Hodeidah University, Al-Hodeidah, Yemen
[c] Department of Mathematics, University of Malakand Chakdara, Dir(L), Pakhtunkhwa, Pakistan

ARTICLE INFO

Article history:
Received 21 April 2020
Revised 27 April 2020
Accepted 4 May 2020
Available online 8 May 2020

MSC:
26A33
34A08
35R11

Keywords:
COVID-19
Attangana-Baleanu derivative
Existence and stability theory
Adams Bashforth method
Fixed point theorem

ABSTRACT

The major purpose of the presented study is to analyze and find the solution for the model of nonlinear fractional differential equations (FDEs) describing the deadly and most parlous virus so-called coronavirus (COVID-19). The mathematical model depending of fourteen nonlinear FDEs is presented and the corresponding numerical results are studied by applying the fractional Adams Bashforth (AB) method. Moreover, a recently introduced fractional nonlocal operator known as Atangana-Baleanu (AB) is applied in order to realize more effectively. For the current results, the fixed point theorems of Krasnoselskii and Banach are hired to present the existence, uniqueness as well as stability of the model. For numerical simulations, the behavior of the approximate solution is presented in terms of graphs through various fractional orders. Finally, a brief discussion on conclusion about the simulation is given to describe how the transmission dynamics of infection take place in society.

1. Introduction

One of the greatest missions given to humankind is to control the environment within which they live. However, the growth of the human population speedily is increasing in relation to different cultures and ways of life. Although Humanity has evolved many species of devices and equipment to obtain a beautiful life. But this excessive development sometimes leads to disasters in the environment. Especially, the use of nutrients, carriages, mobiles, cosmetics, electrified and petroleum equipment, etc, making the environment highly contaminated and infused with viruses.

Newly, the whole world hardship a new coronavirus comprehensive and it was named (COVID-19) which was claimed to flowed first in Wuhan city, China. It has been considered that the origin of COVID-19 is the transportation from animal to human as numerous infected status claimed that they had been to a local fish and wild animal market in Wuhan on 28 November [1]. Soon, some investigators assured that transportation also occurs person to other [2]. This virus dates back to 1965 when Tyrrell and Bynoe were identified when they passage a virus so-called B814 [3]. This virus is found in the cultures of the organs of the human embryonic trachea acquired by the respiratory system of an adult [4].

Because infectious diseases are a major threat to humans as well as the country's economy. A proper understanding of the dynamics of the disease plays a significant role in reducing infection in society.

Application of an appropriate strategy against the disease transportation is another challenge. The mathematical modeling tactic is one of the main tools in order to handle these challenges. Many disease models have been evolved in the existing literature which authorizes us to explore and dominance the prevalence of infectious diseases in a better style. Most of these models rely on classical differential equations. However, in the past few years, it is paying attention that fractional differential equations can be applied to model global phenomena with a greater grade of precision and its applications can be found in various fields for instance dynamic, biology, engineering, control theory, economics, finance and in epidemiology.

* Corresponding author at: Department of Mathematics, University of Malakand Chakdara, Dir(L), Khyber Pakhtunkhwa, Pakistan.
E-mail address: msabdo1977@gmail.com (M.S. Abdo).

https://doi.org/10.1016/j.chaos.2020.109867
0960-0779/

The Fractional calculus transacts with differentiation and integration involving fractional order, which is further outstanding and beneficial than the ordinary integer order in the explanation of the real-world problems, also in the modeling of real phenomena due to a characterization of the memory and hereditary properties [5,6], the integer-order derivative doesn't familiarize the dynamics among two various points. Various types of fractional order or nonlocal derivatives were proposed in the present literature to transact the reduction of a traditional derivative. For instance, based on power-law, Riemann-Liouville introduced the idea of fractional derivative. After that Caputo-Fabrizio in [7] have proposed a new fractional derivative utilizing the exponential kernel. This derivative has a few troubles related to the locality of the kernel. Newly, to overcome Caputo-Fabrizio's problem, Atangana and Baleanu (AB) in [8] have proposed a new modified version of a fractional derivative with the aid of popularized Mittag-Leffler function (MLF) as nonsingular kernel and nonlocal. Since the generalized MLF is used as the kernel and it's guaranteed no singularity, the AB fractional derivative supply a stellar description of memory [9–11].

Because of mathematical models, we can know the rate of change in the COVID-19 how the disease can affect people at risk and quarantined. The area dedicated to the study of the biological model of infectious diseases is a warm area for recent research. Numerous studies on mathematical models were presented to the study of stability theory and the results of existence and improvement of biological models, see [12–24]. For example, Chen, et al., in [12] presented a big mathematical model for simulating the phase-based transmissibility of a novel coronavirus. Hussain et al., in [13] showed the existence and uniqueness of results for the fractional model involving fractional derivative in Atangana-Baleanu sense using Schaefer's and Banach's fixed point theorems. Moreover, they applied the Shehu transform and Picard method to explore the iterative solutions and its stability for the proposed fractional model. A conceptual model for the COVID-19 disease, which effectively catches the time line of this virus outbreak was proposed by Lin et. al. in [14]. In [16] A mathematical modeling and dynamics of a novel (2019-nCoV) are formulated under a fractional model with considering the available infection cases within 7 days. A mathematical model considered by Shaikh et al. [15] to study estimate of the effectiveness of prophylactic measures, prophesying future outbreaks and possibility control strategies of COVID-19.

Due to the success of this operator in modeling infectious diseases, and motivated by the above useful applications of some fractional operators in epidemic mathematical models, in this paper we are studying the dynamics of the novel coronavirus model suggested by Chen et.al., [12] in the form of the system of the nonlinear differential equations involving the AB Caputo fractional derivative:

$$\begin{cases}
{}^{ABC}\mathbb{D}^{\alpha}_{0^+}\mathcal{S}_B(t) = \Lambda_B - m_B\mathcal{S}_B - \beta_B\mathcal{S}_B\mathcal{I}_B,\\
{}^{ABC}\mathbb{D}^{\alpha}_{0^+}\mathcal{E}_B(t) = \beta_B\mathcal{S}_B\mathcal{I}_B - w_B\mathcal{E}_B - m_B\mathcal{E}_B,\\
{}^{ABC}\mathbb{D}^{\alpha}_{0^+}\mathcal{I}_B(t) = m_B\mathcal{E}_B - (\gamma_B + m_B)\mathcal{I}_B,\\
{}^{ABC}\mathbb{D}^{\alpha}_{0^+}\mathcal{R}_B(t) = \gamma_B\mathcal{I}_B - m_B\mathcal{R}_B,\\
{}^{ABC}\mathbb{D}^{\alpha}_{0^+}\mathcal{S}_H(t) = \Lambda_H - m_H\mathcal{S}_H - \beta_{BH}\mathcal{S}_H\mathcal{I}_B - \beta_H\mathcal{S}_H\mathcal{I}_H,\\
{}^{ABC}\mathbb{D}^{\alpha}_{0^+}\mathcal{E}_H(t) = \beta_{BH}\mathcal{S}_H\mathcal{I}_B + \beta_H\mathcal{S}_H\mathcal{I}_H - w_H\mathcal{E}_H - m_H\mathcal{E}_H,\\
{}^{ABC}\mathbb{D}^{\alpha}_{0^+}\mathcal{I}_H(t) = w_H\mathcal{E}_H - (\gamma_H + m_H)\mathcal{I}_H,\\
{}^{ABC}\mathbb{D}^{\alpha}_{0^+}\mathcal{R}_H(t) = \gamma_H\mathcal{I}_H - m_H\mathcal{R}_H,\\
{}^{ABC}\mathbb{D}^{\alpha}_{0^+}\mathcal{S}_\rho = \Lambda_\rho - m_\rho\mathcal{S}_\rho - \beta_\rho\mathcal{S}_\rho(\mathcal{I}_\rho + k\mathcal{A}_\rho) - \beta_w\mathcal{S}_\rho\mathcal{W},\\
{}^{ABC}\mathbb{D}^{\alpha}_{0^+}\mathcal{E}_\rho = \beta_\rho\mathcal{S}_\rho(\mathcal{I}_\rho + k\mathcal{A}_\rho) + \beta_w\mathcal{S}_\rho\mathcal{W}\\
\quad -\big(1-\delta_\rho\big)w_\rho\mathcal{E}_\rho - \delta_\rho w'_\rho\mathcal{E}_\rho - m_\rho\mathcal{E}_\rho,\\
{}^{ABC}\mathbb{D}^{\alpha}_{0^+}\mathcal{I}_\rho = \big(1-\delta_\rho\big)w_\rho\mathcal{E}_\rho - \big(\gamma_\rho + m_\rho\big)\mathcal{I}_\rho,\\
{}^{ABC}\mathbb{D}^{\alpha}_{0^+}\mathcal{A}_\rho = \delta_\rho w'_\rho\mathcal{E}_\rho - \big(\gamma'_\rho + m_\rho\big)\mathcal{A}_\rho,\\
{}^{ABC}\mathbb{D}^{\alpha}_{0^+}\mathcal{R}_\rho = \gamma_\rho\mathcal{I}_\rho + \gamma'_\rho\mathcal{A}_\rho - m_\rho\mathcal{R}_\rho,\\
{}^{ABC}\mathbb{D}^{\alpha}_{0^+}\mathcal{W} = a\mathcal{W}\frac{\mathcal{I}_H}{\mathcal{N}_H} + \mu_\rho\mathcal{I}_\rho + \mu'_\rho\mathcal{A}_\rho - \varepsilon\mathcal{W}
\end{cases} \tag{1}$$

with the initial conditions

$$\begin{cases}
\mathcal{S}_B(0) = \mathcal{S}_{B_0} \geq 0,\ \mathcal{E}_B(0) = \mathcal{E}_{B_0} \geq 0,\ \mathcal{I}_B(0) = \mathcal{I}_{B_0} \geq 0,\\
\mathcal{R}_B(0) = \mathcal{R}_{B_0} \geq 0,\\
\mathcal{S}_H(0) = \mathcal{S}_{H_0} \geq 0,\ \mathcal{E}_H(0) = \mathcal{E}_{H_0} \geq 0,\ \mathcal{I}_H(0) = \mathcal{I}_{H_0} \geq 0,\\
\mathcal{R}_H(0) = \mathcal{R}_{H_0} \geq 0,\\
\mathcal{S}_\rho(0) = \mathcal{S}_{\rho_0} \geq 0,\ \mathcal{E}_\rho(0) = \mathcal{E}_{\rho_0} \geq 0,\ \mathcal{I}_\rho(0) = \mathcal{I}_{\rho_0} \geq 0,\\
\mathcal{A}_\rho(0) = \mathcal{A}_{\rho_0} \geq 0,\ \mathcal{R}_\rho(0) = \mathcal{R}_{\rho_0} \geq 0,\ \mathcal{W}(0) = \mathcal{W}_0 \geq 0,
\end{cases} \tag{2}$$

where ${}^{ABC}\mathbb{D}^{\alpha}_{0^+}$ denotes the Atangana-Baleanu-Caputo fractional derivative of order α. The model is based on the following facts:

1. The bats were split into four closets: $\mathcal{S}_B$ is a susceptible class of bats, $\mathcal{E}_B$ is an exposed class of bats, $\mathcal{I}_B$ is an infected class of bats, and $\mathcal{R}_B$ is a removed class of bats.
2. The hosts were split into four classes: $\mathcal{S}_H$ is a susceptible class of hosts, $\mathcal{E}_H$ is an exposed class of hosts, $\mathcal{I}_H$ is an infected class of hosts, and $\mathcal{R}_H$ is a removed class of hosts.
3. The people were split into six classes: $\mathcal{S}_\rho$ is a susceptible class of people, $\mathcal{E}_\rho$ is an exposed class of people, $\mathcal{I}_\rho$ is an infected class of people, $\mathcal{A}_\rho$ is asymptomatic infected people, $\mathcal{R}_\rho$ is a population of removed people due to death, and $\mathcal{W}$ is the population of the virus in reservoir various.

$\mathcal{S}_{B_0}$, $\mathcal{E}_{B_0}$, $\mathcal{I}_{B_0}$, $\mathcal{R}_{B_0}$,$\mathcal{S}_{H_0}$, $\mathcal{E}_{H_0}$, $\mathcal{I}_{H_0}$, $\mathcal{R}_{H_0}$,$\mathcal{S}_{\rho_0}$, $\mathcal{E}_{\rho_0}$, $\mathcal{I}_{\rho_0}$, $\mathcal{A}_{\rho_0}$, $\mathcal{R}_{\rho_0}$, and $\mathcal{W}_0$ are the initial values corresponding to the three categories.

The parameters of the model (1) are described as follows:

Λ_B denote the birth rate of bats, m_B is the death rate of bats, and β_B is the transmission rate from $\mathcal{I}_B$ to $\mathcal{S}_B$. The parameters $\frac{1}{w_B}$, $\frac{1}{\gamma_B}$, $\frac{1}{w'_\rho}$, and $\frac{1}{\gamma'_\rho}$ are the incubation period of bats, the infectious period of bats, the latent period of people, and the infectious period of asymptomatic infection of people, respectively. Λ_H is Recruitment from total number of hosts and m_H The death rate of hosts. The symbols β_H and β_{BH} represent the transmission rate from $\mathcal{I}_H$ to $\mathcal{S}_H$ and from $\mathcal{I}_B$ to $\mathcal{S}_H$, respectively. Λ_ρ and m_ρ are the birth and death rate parameter of people, respectively. In the proposed model β_ρ and κ are define the transmission rate from $\mathcal{I}_p$ to $\mathcal{S}_p$ and multiple of the transmissibility of $\mathcal{A}_p$ to $\mathcal{I}_p$, respectively. β_ω and β_ρ means the transmission rate from $\mathcal{W}$ to $\mathcal{S}_p$ and from $\mathcal{I}_p$ to $\mathcal{S}_p$, respectively. δ_ρ is the proportion of asymptomatic infection rate of people, γ_ρ is the infectious period of symptomatic infection of people and a is the retail purchases rate of the hosts in the market. The shedding coefficients from $\mathcal{I}_\rho$ to $\mathcal{W}$ and the shedding coefficients from $\mathcal{A}_\rho$ to $\mathcal{W}$ are denoted by μ_ρ and μ'_ρ, respectively. Finally, $\frac{1}{\varepsilon}$ is the lifetime of the virus in $\mathcal{W}$ and $\mathcal{N}_H$ is the total number of hosts.

The major aim of the paper is to demonstrate the existence, uniqueness and Ulam stability of solution for the model (1)-(2) by using some fixed point techniques. Moreover, the numerical simulations via the fractional version of Adams Bashfully technique to approximate the ABC fractional operator are performed, which it is shown that the model displays rich dynamical behaviors through graphical representation of numerical solutions.

This paper is coordinated as follows: Section 1 transacts with the introduction which contains a survey of the literature. Section 2 consists of some foundation preliminaries related the fractional calculus and nonlinear analysis. The existence and Ulam stability results on a proposed model are obtained in Sections 3 and 4. The numerical solution and numerical simulations of the model at hand are presented in Section 5. For the numerical simulation, we use a powerful two step numerical tool called fractional AB method. The concerned numerical method is more powerful than usual Euler method as well Taylor method. Because the mentioned method is faster convergent and stable as compared to Taylor and Euler method which are slowly convergent. For detail about this method, see [32–36].

2. Preliminaries

For short, we will use the following notations

$\mathcal{O}_B = (\mathcal{S}_B, \mathcal{E}_B, \mathcal{I}_B, \mathcal{R}_B)$, $\mathcal{O}_H = (\mathcal{S}_H, \mathcal{I}_H, \mathcal{R}_H)$,
$\mathcal{O}_\rho = (\mathcal{S}_\rho, \mathcal{E}_\rho, \mathcal{I}_\rho, \mathcal{A}_\rho, \mathcal{R}_\rho, \mathcal{W})$.

$$\Psi = (\mathcal{O}_B, \mathcal{O}_H, \mathcal{O}_\rho) = \Big(\mathcal{S}_B, \mathcal{E}_B, \mathcal{I}_B, \mathcal{R}, \mathcal{S}_H, \mathcal{E}_H, \mathcal{I}_H, \mathcal{R}_H, \mathcal{S}_\rho, \mathcal{E}_\rho, \mathcal{I}_\rho, \mathcal{A}_\rho, \mathcal{R}_\rho, \mathcal{W}\Big)$$

For the next analysis, we define Banach space for onward analysis. Let $0 \le t \le T < \infty$, we define the Banach space by using $J = [0, T]$ as $\digamma = C(J, R^{14})$ under the supremum norm given by

$$\|\Psi\| = \sup_{t\in J}\Big\{|\Psi(t)| : \ \Psi \in \digamma\Big\}$$

where

$$|\mathcal{O}_B(t)| = |\mathcal{S}_B(t)| + |\mathcal{E}_B(t)| + |\mathcal{I}_B(t)| + |\mathcal{R}_B(t)|,$$

$$|\mathcal{O}_H(t)| = |\mathcal{S}_H(t)| + |\mathcal{E}_H(t)| + |\mathcal{I}_H(t)| + |\mathcal{R}_H(t)|,$$

$$|\mathcal{O}_\rho(t)| = |\mathcal{S}_\rho(t)| + |\mathcal{E}_\rho(t)| + |\mathcal{I}_\rho(t)| + |\mathcal{A}_\rho(t)| + |\mathcal{R}_\rho(t)| + |\mathcal{W}(t)|,$$

and $\mathcal{S}_\theta, \mathcal{E}_\theta, \mathcal{I}_\theta, \mathcal{A}_\theta, \mathcal{R}_\theta, \mathcal{M} \in C[0, T]$, $\theta \in \{B, H, \rho\}$.

Definition 2.1. [8] Let $\propto \in (0, 1]$ and $\sigma \in H^1(0, T)$. Then the left-sided ABC fractional derivative with the lower limit zero of order $\propto$ for a function σ is defined by

$${}^{ABC}\mathbb{D}^{\propto}_{0^+}\sigma(t) = \frac{\mathcal{N}(\propto)}{1-\propto}\int_0^t \mathbb{E}_\propto\Big(\frac{-\propto}{\propto -1}(t-\theta)^\propto\Big)\sigma'(\theta)d\theta, \quad t > 0,$$

where $\mathcal{N}(\propto)$ is the normalization function which is defined as $\mathcal{N}(\propto) = \frac{\propto}{2-\propto}$, $0 < \propto \le 1$ and satisfies the result $\mathcal{N}(0) = \mathcal{N}(1) = 1$. Further $\mathbb{E}_\propto$ is called the Mittag-Leffler function defined by the series

$$E_\propto(z) = \sum_{k=0}^{\infty}\frac{z^k}{\Gamma(\propto k+1)}, \tag{3}$$

here $Re(\propto) > 0$ and $\Gamma(.)$ is a gamma function.

Definition 2.2. [8] Let $\propto \in (0, 1]$ and $\sigma \in L^1(0, T)$. Then the left-sided ABC fractional integral with the lower limit zero of order $\propto$ for a function σ is defined by

$${}^{ABC}\mathbb{I}^{\propto}_{0^+}\sigma(t) = \frac{1-\propto}{\mathcal{N}(\propto)}\sigma(t) + \frac{\propto}{\mathcal{N}(\propto)}\frac{1}{\Gamma(\propto)}\int_0^t (t-\theta)^{\propto-1}\sigma(\theta)d\theta, \quad t > 0.$$

Definition 2.3. *[8] The Laplace transform of ABC fractional derivative of a function $\sigma(t)$ is given by*

$$\mathcal{L}\Big[{}^{ABC}\mathbb{D}^{\propto}_{0^+}\sigma(t)\Big] = \frac{\mathcal{N}(\propto)}{s^\propto(1-\propto)+\propto}\Big[s^\propto\mathcal{L}[\sigma(t)] - s^{\propto-1}\sigma(0)\Big].$$

Lemma 2.3.1. [8] *The solution of the proposed problem for* $\propto \in (0, 1]$

$$\begin{aligned} {}^{ABC}\mathbb{D}^{\propto}_{0^+}\sigma(t) &= \omega(t), \\ \sigma(0) &= \sigma_0 \end{aligned} \tag{4}$$

is given by

$$\sigma(t) = \sigma_0 + \frac{1-\propto}{\mathcal{N}(\propto)}\omega(t) + \frac{\propto}{\mathcal{N}(\propto)}\frac{1}{\Gamma(\propto)}\int_0^t (t-\theta)^{\propto-1}\omega(\theta)d\theta.$$

Definition 2.4. [25] Let $\digamma$ be a Banach space. The operator Π: $\digamma \to \digamma$ is a Lipschitzian if there exists a constant $\kappa > 0$ such that

$$\|\Pi\Psi_1 - \Pi\Psi_2\| \le \kappa\|\Psi_1 - \Psi_2\|, \text{ for all } \Psi_1, \Psi_2 \in \digamma,$$

here κ is the Lipschitz constant for Π. If $\kappa < 1$ we say that Π is a contraction.

Theorem 2.5. *[25] Let $\digamma$ be a Banach space If $\Pi : \digamma \longrightarrow \digamma$ is a contraction mapping. Then there exists a unique fixed point of Π.*

Theorem 2.6. *[25] (Let $\mathcal{M}$ be a closed, convex, non-empty subset of a Banach space $\digamma$. Suppose that $\mathbb{E}$ and $\mathbb{F}$ map $\mathcal{M}$ into $\digamma$ and that*

(i) $\mathbb{E}u + \mathbb{F}v \in \mathcal{M}$ for all $\Psi_1, \Psi_2 \in \mathcal{M}$;
(ii) $\mathbb{E}$ is compact and continuous;
(iii) $\mathbb{F}$ is a contraction mapping. Then, there exists $\Psi \in \mathcal{M}$ such that $\mathbb{E}\Psi + \mathbb{F}\Psi = \Psi$.

3. Existence of solutions for the proposed model (1)-(2)

Now, we debate the existence and uniqueness results of the model (1)-(2) by utilizing the fixed-point technique. Let us reformulated model (1) in the subsequent appropriate form

$$\begin{cases} {}^{ABC}\mathbb{D}^{\propto}_{0^+}\mathcal{S}_B(t) = \mathcal{F}_1(t, \mathcal{O}_B, \mathcal{O}_H, \mathcal{O}_\rho), \\ {}^{ABC}\mathbb{D}^{\propto}_{0^+}\mathcal{E}_B(t) = \mathcal{F}_2(t, \mathcal{O}_B, \mathcal{O}_H, \mathcal{O}_\rho), \\ {}^{ABC}\mathbb{D}^{\propto}_{0^+}\mathcal{I}_B(t) = \mathcal{F}_3(t, \mathcal{O}_B, \mathcal{O}_H, \mathcal{O}_\rho), \\ {}^{ABC}\mathbb{D}^{\propto}_{0^+}\mathcal{R}_B(t) = \mathcal{F}_4(t, \mathcal{O}_B, \mathcal{O}_H, \mathcal{O}_\rho), \\ {}^{ABC}\mathbb{D}^{\propto}_{0^+}\mathcal{S}_H(t) = \mathcal{F}_5(t, \mathcal{O}_B, \mathcal{O}_H, \mathcal{O}_\rho), \\ {}^{ABC}\mathbb{D}^{\propto}_{0^+}\mathcal{E}_H(t) = \mathcal{F}_6(t, \mathcal{O}_B, \mathcal{O}_H, \mathcal{O}_\rho), \\ {}^{ABC}\mathbb{D}^{\propto}_{0^+}\mathcal{I}_H(t) = \mathcal{F}_7(t, \mathcal{O}_B, \mathcal{O}_H, \mathcal{O}_\rho), \\ {}^{ABC}\mathbb{D}^{\propto}_{0^+}\mathcal{R}_H(t) = \mathcal{F}_8(t, \mathcal{O}_B, \mathcal{O}_H, \mathcal{O}_\rho), \\ {}^{ABC}\mathbb{D}^{\propto}_{0^+}\mathcal{S}_\rho(t) = \mathcal{F}_9(t, \mathcal{O}_B, \mathcal{O}_H, \mathcal{O}_\rho), \\ {}^{ABC}\mathbb{D}^{\propto}_{0^+}\mathcal{E}_\rho(t) = \mathcal{F}_{10}(t, \mathcal{O}_B, \mathcal{O}_H, \mathcal{O}_\rho), \\ {}^{ABC}\mathbb{D}^{\propto}_{0^+}\mathcal{I}_\rho(t) = \mathcal{F}_{11}(t, \mathcal{O}_B, \mathcal{O}_H, \mathcal{O}_\rho), \\ {}^{ABC}\mathbb{D}^{\propto}_{0^+}\mathcal{A}_\rho(t) = \mathcal{F}_{12}(t, \mathcal{O}_B, \mathcal{O}_H, \mathcal{O}_\rho), \\ {}^{ABC}\mathbb{D}^{\propto}_{0^+}\mathcal{R}_\rho(t) = \mathcal{F}_{13}(t, \mathcal{O}_B, \mathcal{O}_H, \mathcal{O}_\rho), \\ {}^{ABC}\mathbb{D}^{\propto}_{0^+}\mathcal{W}(t) = \mathcal{F}_{14}(t, \mathcal{O}_B, \mathcal{O}_H, \mathcal{O}_\rho), \end{cases}$$

where

$$\begin{cases} \mathcal{F}_1(t, \mathcal{O}_B, \mathcal{O}_H, \mathcal{O}_\rho) = \Lambda_B - m_B\mathcal{S}_B - \beta_B\mathcal{S}_B\mathcal{I}_B, \\ \mathcal{F}_2(t, \mathcal{O}_B, \mathcal{O}_H, \mathcal{O}_\rho) = \beta_B\mathcal{S}_B\mathcal{I}_B - w_B\mathcal{E}_B - m_B\mathcal{E}_B, \\ \mathcal{F}_3(t, \mathcal{O}_B, \mathcal{O}_H, \mathcal{O}_\rho) = m_B\mathcal{E}_B - (\gamma_B + m_B)\mathcal{I}_B, \\ \mathcal{F}_4(t, \mathcal{O}_B, \mathcal{O}_H, \mathcal{O}_\rho) = \gamma_B\mathcal{I}_B - m_B\mathcal{R}_B, \\ \mathcal{F}_5(t, \mathcal{O}_B, \mathcal{O}_H, \mathcal{O}_\rho) = \Lambda_H - m_H\mathcal{S}_H - \beta_{BH}\mathcal{S}_H\mathcal{I}_B - \beta_H\mathcal{S}_H\mathcal{I}_H, \\ \mathcal{F}_6(t, \mathcal{O}_B, \mathcal{O}_H, \mathcal{O}_\rho) = \beta_{BH}\mathcal{S}_H\mathcal{I}_B + \beta_H\mathcal{S}_H\mathcal{I}_H - w_H\mathcal{E}_H - m_H\mathcal{E}_H, \\ \mathcal{F}_7(t, \mathcal{O}_B, \mathcal{O}_H, \mathcal{O}_\rho) = w_H\mathcal{E}_H - (\gamma_H + m_H)\mathcal{I}_H, \\ \mathcal{F}_8(t, \mathcal{O}_B, \mathcal{O}_H, \mathcal{O}_\rho) = \gamma_H\mathcal{I}_H - m_H\mathcal{R}_H, \\ \mathcal{F}_9(t, \mathcal{O}_B, \mathcal{O}_H, \mathcal{O}_\rho) = \Lambda_\rho - m_\rho\mathcal{S}_\rho - \beta_\rho\mathcal{S}_\rho(\mathcal{I}_\rho + k\mathcal{A}_\rho) \\ \quad -\beta_w\mathcal{S}_\rho\mathcal{W}, \\ \mathcal{F}_{10}(t, \mathcal{O}_B, \mathcal{O}_H, \mathcal{O}_\rho) = \beta_\rho\mathcal{S}_\rho(\mathcal{I}_\rho + k\mathcal{A}_\rho) + \beta_w\mathcal{S}_\rho\mathcal{W} \\ \quad -\big(1-\delta_\rho\big)w_\rho\mathcal{E}_\rho - \delta_\rho w'_\rho\mathcal{E}_\rho - m_\rho\mathcal{E}_\rho, \\ \mathcal{F}_{11}(t, \mathcal{O}_B, \mathcal{O}_H, \mathcal{O}_\rho) = \big(1-\delta_\rho\big)w_\rho\mathcal{E}_\rho - \big(\gamma_\rho + m_\rho\big)\mathcal{I}_\rho, \\ \mathcal{F}_{12}(t, \mathcal{O}_B, \mathcal{O}_H, \mathcal{O}_\rho) = \delta_\rho w'_\rho\mathcal{E}_\rho - \big(\gamma'_\rho + m_\rho\big)\mathcal{A}_\rho, \\ \mathcal{F}_{13}(t, \mathcal{O}_B, \mathcal{O}_H, \mathcal{O}_\rho) = \gamma_\rho\mathcal{I}_\rho + \gamma'_\rho\mathcal{A}_\rho - m_\rho\mathcal{R}_\rho, \\ \mathcal{F}_{14}(t, \mathcal{O}_B, \mathcal{O}_H, \mathcal{O}_\rho) = a\mathcal{W}\frac{\mathcal{I}_H}{\mathcal{N}_H} + \mu_\rho\mathcal{I}_\rho + \mu'_\rho\mathcal{A}_\rho - \varepsilon\mathcal{W} \end{cases} \tag{5}$$

We take our system as by using (1)

$$\begin{cases} {}^{ABC}\mathbb{D}^{\propto}_{0^+}\Psi(t) = \mathcal{H}(t, \Psi(t)), \\ \Psi(0) = \Psi_0 \ge 0, \end{cases} \tag{6}$$

where

$$\begin{cases} \Psi(t) := \big(\mathcal{O}_B, \mathcal{O}_H, \mathcal{O}_\rho\big)^T = (\mathcal{S}_B, \mathcal{E}_B, \mathcal{I}_B, \mathcal{R}_B, \mathcal{S}_H, \mathcal{E}_H, \mathcal{I}_H, \\ \quad \mathcal{R}_H, \mathcal{S}_\rho, \mathcal{E}_\rho, \mathcal{I}_\rho, \mathcal{A}_\rho, \mathcal{R}_\rho, \mathcal{W})^T, \\ \Psi_0 := \big(\mathcal{O}_{B_0}, \mathcal{O}_{H_0}, \mathcal{O}_{\rho_0}\big)^T = \big(\mathcal{S}_{B_0}, \mathcal{E}_{B_0}, \mathcal{I}_{B_0}, \mathcal{R}_{B_0}, \mathcal{S}_{H_0}, \mathcal{E}_{H_0}, \\ \quad \mathcal{I}_{H_0}, \mathcal{R}_{H_0}, \mathcal{S}_{\rho_0}, \mathcal{E}_{\rho_0}, \mathcal{I}_{\rho_0}, \mathcal{A}_{\rho_0}, \mathcal{R}_{\rho_0}, \mathcal{W}_0\big)^T, \\ \mathcal{H}(t, \Psi(t)) = \big(\mathcal{F}_\ell(t, \mathcal{O}_B, \mathcal{O}_H, \mathcal{O}_\rho)\big)^T, \quad \ell = 1, 2, 3, \ldots, 14, \end{cases} \tag{7}$$

Here the symbol A^T denotes the transpose operation. Utilizing Lemma 2.3.1, the model (6) can be turned to the fractional integral equation in the sense of AB fractional integral as follows

$$\Psi(t) = \Psi_0 + \frac{1-\alpha}{\mathcal{N}(\alpha)}\mathcal{H}(t,\Psi(t)) + \frac{\alpha}{\mathcal{N}(\alpha)}\frac{1}{\Gamma(\alpha)}\int_0^t (t-\zeta)^{\alpha-1}\mathcal{H}(\zeta,\Psi(\zeta))d\zeta. \quad (8)$$

Expressing some growth condition and Lipschitzian assumption for existence uniqueness as:

(Hypothesis 1) There exists two constants $\mu_{\mathcal{H}}, \eta_{\mathcal{H}}$ such that

$$|\mathcal{H}(t,\Psi(t))| \le \mu_{\mathcal{H}}|\Psi| + \eta_{\mathcal{H}}, \quad t \in [0,T].$$

(Hypothesis 2) There exists constants $L_{\mathcal{H}} > 0$ such that

$$|\mathcal{H}(t,\Psi_1) - \mathcal{H}(t,\Psi_2)| \le L_{\mathcal{H}}|\Psi_1 - \Psi_2|;$$

for each $\Psi \in \mathcal{F}$ and $t \in [0,T]$.

Theorem 3.1. *Let the hypotheses 1,2 hold. The Integral equation (8) which equivalent of the considered model (1)-(2) has at least one solution if* $\frac{1-\alpha}{\mathcal{N}(\alpha)}L_{\mathcal{H}}, \Theta_1 < 1$ *where*

$$\Theta_1 := \left[\frac{1-\alpha}{\mathcal{N}(\alpha)} + \frac{T^\alpha}{\mathcal{N}(\alpha)\Gamma(\alpha)}\right]\mu_{\mathcal{H}} < 1. \quad (9)$$

Theorem 3.2.

Proof. *Consider* $\mathbb{B}_\lambda = \{\Psi \in \mathcal{F} : \|\Psi\| \le \lambda\}$ *is closed convex set with* $\lambda \ge \frac{\Theta_2}{1-\Theta_1}$, *where*

$$\Theta_2 := |\Psi_0| + \left[\frac{1-\alpha}{\mathcal{N}(\alpha)} + \frac{T^\alpha}{\mathcal{N}(\alpha)\Gamma(\alpha)}\right]\eta_{\mathcal{H}}. \quad (10)$$

We define the operators Π_1 *and* Π_2 *as*

$$\Pi_1\Psi(t) = \Psi_0 + \frac{1-\alpha}{\mathcal{N}(\alpha)}\mathcal{H}(t,\Psi(t)),$$

$$\Pi_2\Psi(t) = \frac{\alpha}{\mathcal{N}(\alpha)}\frac{1}{\Gamma(\alpha)}\int_0^t (t-\zeta)^{\alpha-1}\mathcal{H}(\zeta,\Psi(\zeta))d\zeta,$$

where $\mathcal{F} = \Pi_1 + \Pi_2$. *Now, we offer the proof in several steps as:*

Step1: $\Pi_1\Psi_1 + \Pi_2\Psi_2 \in \mathbb{B}_\lambda$, *for* $\Psi_1, \Psi_2 \in \mathbb{B}_\lambda$.

Indeed, From (Hypothesis 1) and equations (9),(10), we obtain

$$\begin{aligned}\|\Pi_1\Psi_1 + \Pi_2\Psi_2\| &\le \max_{t\in[0,T]}\left\{|\Psi_0| + \frac{1-\alpha}{\mathcal{N}(\alpha)}|\mathcal{H}(t,\Psi(t))| + \frac{\alpha}{\mathcal{N}(\alpha)}\frac{1}{\Gamma(\alpha)}\int_0^t (t-\zeta)^{\alpha-1}|\mathcal{H}(\zeta,\Psi(\zeta))|d\zeta\right\}\\ &\le \left\{|\Psi_0| + \frac{1-\alpha}{\mathcal{N}(\alpha)}[\mu_{\mathcal{H}}\|\Psi\| + \eta_{\mathcal{H}}] + \frac{\alpha}{\mathcal{N}(\alpha)}\frac{1}{\Gamma(\alpha)}\int_0^t (t-\zeta)^{\alpha-1}[\mu_{\mathcal{H}}\|\Psi\| + \eta_{\mathcal{H}}]d\zeta\right\}\\ &= |\Psi_0| + \left[\frac{1-\alpha}{\mathcal{N}(\alpha)} + \frac{T^\alpha}{\mathcal{N}(\alpha)\Gamma(\alpha)}\right]\eta_{\mathcal{H}} + \left[\frac{1-\alpha}{\mathcal{N}(\alpha)} + \frac{T^\alpha}{\mathcal{N}(\alpha)\Gamma(\alpha)}\right]\mu_{\mathcal{H}}\lambda\\ &= \Theta_2 + \Theta_1\lambda \le \lambda.\end{aligned}$$

This confirms that $\Pi_1\Psi_1 + \Pi_2\Psi_2 \in \mathbb{B}_\lambda$.

Step1: we show that Π_1 *is contraction.*

Let $\Psi, \Psi^* \in \mathbb{B}_\lambda$. *By (Hypothesis 2), we have*

$$\begin{aligned}\|\Pi_1\Psi - \Pi_1\Psi^*\| &= \max_{t\in[0,T]}\frac{1-\alpha}{\mathcal{N}(\alpha)}|\mathcal{H}(t,\Psi(t)) - \mathcal{H}(t,\Psi^*(t))|\\ &\le \frac{1-\alpha}{\mathcal{N}(\alpha)}L_{\mathcal{H}}\max_{t\in[0,T]}|\Psi(t) - \Psi^*(t)|\\ &\le \frac{1-\alpha}{\mathcal{N}(\alpha)}L_{\mathcal{H}}\|\Psi - \Psi^*\|.\end{aligned}$$

As $\frac{1-\alpha}{\mathcal{N}(\alpha)}L_{\mathcal{H}} < 1$, Π_1 *is contraction mapping.*

Step 3: We show that Π_2 *is relatively compact.*

To prove that, we show that Π_2 *is continuous, uniform bounded, and equicontinuous.*

Since $\Psi(t)$ *is continuous, then* $\Pi_2\Psi(t)$ *is continuous. Next, let* $\Psi \in \mathbb{B}_\lambda$, *we have*

$$\begin{aligned}\|\Pi_2\Psi\| &\le \max_{t\in[0,T]}\frac{\alpha}{\mathcal{N}(\alpha)}\frac{1}{\Gamma(\alpha)}\int_0^t (t-\zeta)^{\alpha-1}|\mathcal{H}(\zeta,\Psi(\zeta))|d\zeta\\ &\le \frac{\alpha}{\mathcal{N}(\alpha)\Gamma(\alpha)}\int_0^t (t-\zeta)^{\alpha-1}\left[\mu_{\mathcal{H}}\max_{t\in[0,T]}|\Psi| + \eta_{\mathcal{H}}\right]d\zeta\\ &\le \frac{\alpha}{\mathcal{N}(\alpha)\Gamma(\alpha)}\int_0^t (t-\zeta)^{\alpha-1}[\mu_{\mathcal{H}}\|\Psi\| + \eta_{\mathcal{H}}]d\zeta\\ &\le \frac{T^\alpha}{\mathcal{N}(\alpha)\Gamma(\alpha)}[\mu_{\mathcal{H}}\lambda + \eta_{\mathcal{H}}].\end{aligned}$$

Hence Π_2 *is uniformly bounded on* $\mathbb{B}_\lambda$. *Finally, we show that* Π_2 *equicontinuous. Let* $\Psi \in \mathbb{B}_\lambda$ *and* $t_1, t_2 \in [0,T]$ *such that* $t_1 < t_2$. *Then*

$$\begin{aligned}&\|\Pi_2\Psi(t_2) - \Pi_2\Psi(t_1)\|\\ &\le \frac{\alpha}{\mathcal{N}(\alpha)}\frac{1}{\Gamma(\alpha)}\int_{t_1}^{t_2}(t_2-\zeta)^{\alpha-1}|\mathcal{H}(\zeta,\Psi(\zeta))|d\zeta\\ &\quad + \frac{\alpha}{\mathcal{N}(\alpha)}\frac{1}{\Gamma(\alpha)}\int_0^{t_1}(t_1-\zeta)^{\alpha-1} - (t_2-\zeta)^{\alpha-1}|\mathcal{H}(\zeta,\Psi(\zeta))|d\zeta\\ &\le \frac{[\mu_{\mathcal{H}}\lambda + \eta_{\mathcal{H}}]}{\mathcal{N}(\alpha)\Gamma(\alpha)}[(t_2-t_1)^\alpha + (t_1^\alpha - t_2^\alpha) + (t_2-t_1)^\alpha]\\ &= \frac{2[\mu_{\mathcal{H}}\lambda + \eta_{\mathcal{H}}]}{\mathcal{N}(\alpha)\Gamma(\alpha)}[(t_2-t_1)^\alpha].\end{aligned}$$

As $t_1 \to t_2$ *the right-hand side of the above inequality tends to zero. Consequently, by Arzelá–Ascoli theorem,* Π_2 *is relatively compact and so completely continuous. Thus by Theorem 2.6, the integral equation (8) has at least one solution and consequently the model under consideration has at least one solution.* □

Theorem 3.3. *Under Hypothesis 2, the integral equation (8) has unique solution which yields that the model (1)-(2) has unique result if*

$$\Theta_3 := \left(\frac{1-\alpha}{\mathcal{N}(\alpha)} + \frac{T^\alpha}{\mathcal{N}(\alpha)\Gamma(\alpha)}\right)L_{\mathcal{H}} < 1. \quad (11)$$

Proof. Let the operator Π: $\mathcal{F} \to \mathcal{F}$ defined by

$$\Pi\Psi(t) = \Psi_0 + \frac{1-\alpha}{\mathcal{N}(\alpha)}\mathcal{H}(t,\Psi(t)) + \frac{\alpha}{\mathcal{N}(\alpha)}\frac{1}{\Gamma(\alpha)}\int_0^t (t-\zeta)^{\alpha-1}\mathcal{H}(\zeta,\Psi(\zeta))d\zeta. \quad (12)$$

Let Ψ and Ψ^* in $\mathcal{F}$ and $t \in [0,T]$. Then

$$\begin{aligned}&\|\Pi\Psi(t) - \Pi\Psi^*(t)\|\\ &\le \max_{t\in[0,T]}\frac{1-\alpha}{\mathcal{N}(\alpha)}|\mathcal{H}(t,\Psi(t)) - \mathcal{H}(t,\Psi^*(t))|\\ &\quad + \max_{t\in[0,T]}\frac{\alpha}{\mathcal{N}(\alpha)}\frac{1}{\Gamma(\alpha)}\int_0^t (t-\zeta)^{\alpha-1}|\mathcal{H}(\zeta,\Psi(\zeta)) - \mathcal{H}(\zeta,\Psi^*(\zeta))|d\zeta\\ &\le \left(\frac{1-\alpha}{\mathcal{N}(\alpha)} + \frac{T^\alpha}{\mathcal{N}(\alpha)\Gamma(\alpha)}\right)L_{\mathcal{H}}\|\Psi - \Psi^*\|.\end{aligned}$$

Due to (11), Π is contraction. Therefore the integral equation (8) has unique solution. Hence our model (1)-(2) has unique solution. □

4. Ulam-Hyers stability

The notion of Ulam stability was initiated by Ulam [26,27]. Then aforesaid stability has been scrutinized for classical fractional derivatives in many of the research articles, we refer to some of them like [28–31]. Additionally, since stability is a prerequisite in respect of approximate solution, so we endeavor on Ulam type stability for the model (1) via using nonlinear functional analysis.

Definition 4.1. System (1)-(2) is U-H stable if there exists $\lambda > 0$ with the following property: For some $\epsilon > 0$, and each $\widetilde{\Psi} \in \digamma$, if

$$\left\{\left|{}^{ABC}\mathbb{D}_{0^+}^{\propto}\widetilde{\Psi}(t) - \mathcal{H}(t,\widetilde{\Psi}(t))\right| \le \epsilon, \tag{13}$$

then there exists $\Psi \in \digamma$ satisfying the model (1) with the following initial condition

$$\Psi(0) = \widetilde{\Psi}(0), \tag{14}$$

such that

$$\left\|\widetilde{\Psi} - \Psi\right\| \le \lambda\epsilon.$$

where

$$\begin{cases} \Psi(t) := \left(\widetilde{\mathcal{O}_B}, \widetilde{\mathcal{O}_H}, \widetilde{\mathcal{O}_\rho}\right)^T = \left(\widetilde{\mathcal{S}_B}, \widetilde{\mathcal{E}_B}, \widetilde{\mathcal{I}_B}, \widetilde{\mathcal{R}_B}, \widetilde{\mathcal{S}_H}, \widetilde{\mathcal{E}_H}, \widetilde{\mathcal{I}_H}, \widetilde{\mathcal{R}_H}, \right. \\ \quad \left. \widetilde{\mathcal{S}_\rho}, \widetilde{\mathcal{E}_\rho}, \widetilde{\mathcal{I}_\rho}, \widetilde{\mathcal{A}_\rho}, \widetilde{\mathcal{R}_\rho}, \widetilde{\mathcal{W}}\right)^T, \\ \Psi_0 := \left(\widetilde{\mathcal{O}_{B_0}}, \widetilde{\mathcal{O}_{H_0}}, \widetilde{\mathcal{O}_{\rho_0}}\right)^T = \left(\widetilde{\mathcal{S}_{B_0}}, \widetilde{\mathcal{E}_{B_0}}, \widetilde{\mathcal{I}_{B_0}}, \widetilde{\mathcal{R}_{B_0}}, \widetilde{\mathcal{S}_{H_0}}, \widetilde{\mathcal{E}_{H_0}}, \widetilde{\mathcal{I}_{H_0}}, \right. \\ \quad \left. \widetilde{\mathcal{R}_{H_0}}, \widetilde{\mathcal{S}_{\rho_0}}, \widetilde{\mathcal{E}_{\rho_0}}, \widetilde{\mathcal{I}_{\rho_0}}, \widetilde{\mathcal{A}_{\rho_0}}, \widetilde{\mathcal{R}_{\rho_0}}, \widetilde{\mathcal{W}_0}\right)^T, \\ \mathcal{H}(t,\widetilde{\Psi}(t)) = \left(\mathcal{F}_\ell(t, \widetilde{\mathcal{O}_B}, \widetilde{\mathcal{O}_H}, \widetilde{\mathcal{O}_\rho})\right)^T, \quad \ell = 1,2,3,\ldots,14, \\ \epsilon = \max(\epsilon_1,\epsilon_2,\epsilon_3,\ldots,\epsilon_{14})^T, \quad \lambda = \max(\lambda_1,\lambda_2,\lambda_3,\ldots,\lambda_{14})^T, \end{cases}$$

Remark 1. Consider a small perturbation $g \in C[0, T]$ such that $g(0) = 0$ comply with the following properties.

1. $|g(t)| \le \epsilon$, for $t \in [0, T]$ and $\epsilon_1 > 0$.
2. For $t \in [0, T]$ we have the following model

$${}^{ABC}\mathbb{D}_{0^+}^{\propto}\widetilde{\Psi}(t) = \mathcal{H}(t,\widetilde{\Psi}(t)) + g(t),$$

where $g(t) = (g_1(t), g_2(t), g_3(t), \ldots, g_{14}(t))^T$.

Lemma 4.1.1. *The solution of the perturbed problem*

$$\begin{cases} {}^{ABC}\mathbb{D}_{0^+}^{\propto}\widetilde{\Psi}(t) = \mathcal{H}(t,\widetilde{\Psi}(t)) + g(t), \\ \widetilde{\Psi}(0) = \widetilde{\Psi}_0 \end{cases} \tag{15}$$

satisfies the given relation

$$\left|\widetilde{\Psi}_g(t) - \widetilde{\Psi}(t)\right| \le \kappa\epsilon,$$

where $\widetilde{\Psi}_g(t)$ is a solution of (15), $\widetilde{\Psi}(t)$ is satisfies (13-a), and $\kappa := \left(\frac{\Gamma(\propto)(1-\propto)+T^{\propto}}{\mathcal{N}(\propto)\Gamma(\propto)}\right)$.

Proof. Thanks to Remark 1 (2), and Lemma 2.3.1, the solution of (15) is given by

$$\widetilde{\Psi}_g(t) = \begin{cases} \widetilde{\Psi}_0 + \frac{1-\propto}{\mathcal{N}(\propto)}\mathcal{H}(t,\widetilde{\Psi}(t)) \\ \quad + \frac{\propto}{\mathcal{N}(\propto)}\frac{1}{\Gamma(\propto)}\int_0^t (t-\zeta)^{\propto-1}\mathcal{H}(\zeta,\widetilde{\Psi}(\zeta))d\zeta \\ \quad + \frac{1-\propto}{\mathcal{N}(\propto)}g(t) + \frac{\propto}{\mathcal{N}(\propto)}\frac{1}{\Gamma(\propto)}\int_0^t (t-\zeta)^{\propto-1}g(\zeta)d\zeta. \end{cases}$$

Also, we have

$$\widetilde{\Psi}(t) = \widetilde{\Psi}_0 + \frac{1-\propto}{\mathcal{N}(\propto)}\mathcal{H}(t,\widetilde{\Psi}(t)) + \frac{\propto}{\mathcal{N}(\propto)}\frac{1}{\Gamma(\propto)}\int_0^t (t-\zeta)^{\propto-1}\mathcal{H}(\zeta,\widetilde{\Psi}(\zeta))d\zeta.$$

It follows from Remark 1(1) that

$$\begin{aligned} &\left|\widetilde{\Psi}_g(t) - \widetilde{\Psi}(t)\right| \\ &\le \frac{1-\propto}{\mathcal{N}(\propto)}|g(t)| + \frac{\propto}{\mathcal{N}(\propto)}\frac{1}{\Gamma(\propto)}\int_0^t (t-\zeta)^{\propto-1}|g(\zeta)|d\zeta \\ &\le \left(\frac{\Gamma(\propto)(1-\propto)+T^{\propto}}{\mathcal{N}(\propto)\Gamma(\propto)}\right)\epsilon \\ &= \kappa\epsilon. \end{aligned}$$

□

Theorem 4.2. *Under the presumptions of Theorem 3.3. Then the model (1)-(2) will be U-H stable in $\digamma$.*

Proof. Let $\widetilde{\Psi} \in \digamma$ be the solution of the inequality (13-a) and the function $\Psi \in \digamma$ is a unique solution of equation (1-a) with the condition

$$\Psi(0) = \widetilde{\Psi}(0). \tag{16}$$

That is

$$\Psi(t) = \Psi_0 + \frac{1-\propto}{\mathcal{N}(\propto)}\mathcal{H}(t,\Psi(t)) + \frac{\propto}{\mathcal{N}(\propto)}\frac{1}{\Gamma(\propto)}\int_0^t (t-\zeta)^{\propto-1}\mathcal{H}(\zeta,\Psi(\zeta))d\zeta \tag{17}$$

Due to (16), $\Psi_0 = \widetilde{\Psi}_0$, the equation (17) becomes

$$\Psi(t) = \widetilde{\Psi}_0 + \frac{1-\propto}{\mathcal{N}(\propto)}\mathcal{H}(t,\Psi(t)) + \frac{\propto}{\mathcal{N}(\propto)}\frac{1}{\Gamma(\propto)}\int_0^t (t-\zeta)^{\propto-1}\mathcal{H}(\zeta,\Psi(\zeta))d\zeta.$$

Thus by Hypothesis 1 and Lemma 4.1.1, we obtain

$$\begin{aligned} \left|\widetilde{\Psi}(t) - \Psi(t)\right| &\le \left|\widetilde{\Psi}(t) - \widetilde{\Psi}_g(t)\right| + \left|\widetilde{\Psi}_g(t) - \Psi(t)\right| \\ &\le \kappa\epsilon + \frac{1-\propto}{\mathcal{N}(\propto)}\left|\mathcal{H}(t,\widetilde{\Psi}(t)) - \mathcal{H}(t,\Psi(t))\right| \\ &\quad + \frac{\propto}{\mathcal{N}(\propto)}\frac{1}{\Gamma(\propto)} \\ &\quad \int_0^t (t-\zeta)^{\propto-1}\left|\mathcal{H}(t,\widetilde{\Psi}(t)) - \mathcal{H}(t,\Psi(t))\right|d\zeta + \kappa\epsilon \\ &\le 2\kappa\epsilon + \left(\frac{1-\propto}{\mathcal{N}(\propto)} + \frac{T^{\propto}}{\mathcal{N}(\propto)\Gamma(\propto)}\right)L_{\mathcal{H}}\left\|\widetilde{\Psi} - \Psi\right\|. \end{aligned}$$

which implies

$$\left\|\widetilde{\Psi} - \Psi\right\| \le \frac{2\kappa\epsilon}{1-\Theta_3},$$

Due to $\Theta_3 < 1$. For $\lambda = \frac{2\kappa}{1-\Theta_3}$, we get $\left\|\widetilde{\Psi} - \Psi\right\| \le \lambda\epsilon$.

Hence the model (1)-(2) is U-H stable. □

5. Numerical approach

In this part, we give approximation solutions of the ABC fractional model (1)-(2). Then the numerical simulations are acquired via the suggested scheme. To this aim, we employ the modified fractional version for Adams Bashforth technique to approximate the fractional integral in the sense AB.

Using the initial conditions and fractional integral operator, we convert model (1) into the integral equations

$$\begin{cases} \mathcal{S}_B(t) - \mathcal{S}_B(0) = {}^{ABC}\mathbb{I}_{0^+}^{\propto}\mathcal{P}_1(t,\mathcal{S}_B(t)), \\ \mathcal{E}_B(t) - \mathcal{E}_B(0) = {}^{ABC}\mathbb{I}_{0^+}^{\propto}\mathcal{P}_2(t,\mathcal{E}_B(t)), \\ \mathcal{I}_B(t) - \mathcal{I}_B(0) = {}^{ABC}\mathbb{I}_{0^+}^{\propto}\mathcal{P}_3(t,\mathcal{I}_B(t)), \\ \mathcal{R}_B(t) - \mathcal{R}_B(0) = {}^{ABC}\mathbb{I}_{0^+}^{\propto}\mathcal{P}_4(t,\mathcal{R}_B(t)), \\ \mathcal{S}_H(t) - \mathcal{S}_H(0) = {}^{ABC}\mathbb{I}_{0^+}^{\propto}\mathcal{P}_5(t,\mathcal{S}_H(t)), \\ \mathcal{E}_H(t) - \mathcal{E}_H(0) = {}^{ABC}\mathbb{I}_{0^+}^{\propto}\mathcal{P}_6(t,\mathcal{E}_H(t)), \\ \mathcal{I}_H(t) - \mathcal{I}_H(0) = {}^{ABC}\mathbb{I}_{0^+}^{\propto}\mathcal{P}_7(t,\mathcal{I}_H(t)), \\ \mathcal{R}_H(t) - \mathcal{R}_H(0) = {}^{ABC}\mathbb{I}_{0^+}^{\propto}\mathcal{P}_8(t,\mathcal{R}_H(t)), \\ \mathcal{S}_\rho(t) - \mathcal{S}_\rho(0) = {}^{ABC}\mathbb{I}_{0^+}^{\propto}\mathcal{P}_9(t,\mathcal{S}_\rho(t)), \\ \mathcal{E}_\rho(t) - \mathcal{E}_\rho(0) = {}^{ABC}\mathbb{I}_{0^+}^{\propto}\mathcal{P}_{10}(t,\mathcal{E}_\rho(t)), \\ \mathcal{I}_\rho(t) - \mathcal{I}_\rho(0) = {}^{ABC}\mathbb{I}_{0^+}^{\propto}\mathcal{P}_{11}(t,\mathcal{I}_\rho(t)), \\ \mathcal{A}_\rho(t) - \mathcal{A}_\rho(0) = {}^{ABC}\mathbb{I}_{0^+}^{\propto}\mathcal{P}_{12}(t,\mathcal{A}_\rho(t)), \\ \mathcal{R}_\rho(t) - \mathcal{R}_\rho(0) = {}^{ABC}\mathbb{I}_{0^+}^{\propto}\mathcal{P}_{13}(t,\mathcal{R}_\rho(t)), \\ \mathcal{W}(t) - \mathcal{W}(0) = {}^{ABC}\mathbb{I}_{0^+}^{\propto}\mathcal{P}_{14}(t,\mathcal{W}(t)), \end{cases} \tag{18}$$

which implies

$$\begin{cases}
\mathcal{S}_B(t)-\mathcal{S}_B(0)=\frac{1-\alpha}{\mathcal{N}(\alpha)}\mathcal{P}_1(t,\mathcal{S}_B(t))\\
\quad+\frac{\alpha}{\mathcal{N}(\alpha)}\frac{1}{\Gamma(\alpha)}\int_0^t(t-\zeta)^{\alpha-1}\mathcal{P}_1(\zeta,\mathcal{S}_B(\zeta))d\zeta,\\
\mathcal{E}_B(t)-\mathcal{E}_B(0)=\frac{1-\alpha}{\mathcal{N}(\alpha)}\mathcal{P}_2(t,\mathcal{E}_B(t))\\
\quad+\frac{\alpha}{\mathcal{N}(\alpha)}\frac{1}{\Gamma(\alpha)}\int_0^t(t-\zeta)^{\alpha-1}\mathcal{P}_2(\zeta,\mathcal{E}_B(\zeta))d\zeta,\\
\mathcal{I}_B(t)-\mathcal{I}_B(0)=\frac{1-\alpha}{\mathcal{N}(\alpha)}\mathcal{P}_3(t,\mathcal{I}_B(t))\\
\quad+\frac{\alpha}{\mathcal{N}(\alpha)}\frac{1}{\Gamma(\alpha)}\int_0^t(t-\zeta)^{\alpha-1}\mathcal{P}_3(\zeta,\mathcal{I}_B(\zeta))d\zeta,\\
\mathcal{R}_B(t)-\mathcal{R}_B(0)=\frac{1-\alpha}{\mathcal{N}(\alpha)}\mathcal{P}_4(t,\mathcal{R}_B(t))\\
\quad+\frac{\alpha}{\mathcal{N}(\alpha)}\frac{1}{\Gamma(\alpha)}\int_0^t(t-\zeta)^{\alpha-1}\mathcal{P}_4(\zeta,\mathcal{R}_B(\zeta))d\zeta,\\
\mathcal{S}_H(t)-\mathcal{S}_H(0)=\frac{1-\alpha}{\mathcal{N}(\alpha)}\mathcal{P}_5(t,\mathcal{S}_H(t))\\
\quad+\frac{\alpha}{\mathcal{N}(\alpha)}\frac{1}{\Gamma(\alpha)}\int_0^t(t-\zeta)^{\alpha-1}\mathcal{P}_5(\zeta,\mathcal{S}_H(\zeta))d\zeta,\\
\mathcal{E}_H(t)-\mathcal{E}_H(0)=\frac{1-\alpha}{\mathcal{N}(\alpha)}\mathcal{P}_6(t,\mathcal{E}_H(t))\\
\quad+\frac{\alpha}{\mathcal{N}(\alpha)}\frac{1}{\Gamma(\alpha)}\int_0^t(t-\zeta)^{\alpha-1}\mathcal{P}_6(\zeta,\mathcal{E}_H(\zeta))d\zeta,\\
\mathcal{I}_H(t)-\mathcal{I}_H(0)=\frac{1-\alpha}{\mathcal{N}(\alpha)}\mathcal{P}_7(t,\mathcal{I}_H(t))\\
\quad+\frac{\alpha}{\mathcal{N}(\alpha)}\frac{1}{\Gamma(\alpha)}\int_0^t(t-\zeta)^{\alpha-1}\mathcal{P}_7(\zeta,\mathcal{I}_H(\zeta))d\zeta,\\
\mathcal{R}_H(t)-\mathcal{R}_H(0)=\frac{1-\alpha}{\mathcal{N}(\alpha)}\mathcal{P}_8(t,\mathcal{R}_H(t))\\
\quad+\frac{\alpha}{\mathcal{N}(\alpha)}\frac{1}{\Gamma(\alpha)}\int_0^t(t-\zeta)^{\alpha-1}\mathcal{P}_8(\zeta,\mathcal{R}_H(\zeta))d\zeta,\\
\mathcal{S}_\rho(t)-\mathcal{S}_\rho(0)=\frac{1-\alpha}{\mathcal{N}(\alpha)}\mathcal{P}_9(t,\mathcal{S}_\rho(t))\\
\quad+\frac{\alpha}{\mathcal{N}(\alpha)}\frac{1}{\Gamma(\alpha)}\int_0^t(t-\zeta)^{\alpha-1}\mathcal{P}_9(\zeta,\mathcal{S}_\rho(\zeta))d\zeta,\\
\mathcal{E}_\rho(t)-\mathcal{E}_\rho(0)=\frac{1-\alpha}{\mathcal{N}(\alpha)}\mathcal{P}_{10}(t,\mathcal{E}_\rho(t))\\
\quad+\frac{\alpha}{\mathcal{N}(\alpha)}\frac{1}{\Gamma(\alpha)}\int_0^t(t-\zeta)^{\alpha-1}\mathcal{P}_{10}(\zeta,\mathcal{E}_\rho(\zeta))d\zeta,\\
\mathcal{I}_\rho(t)-\mathcal{I}_\rho(0)=\frac{1-\alpha}{\mathcal{N}(\alpha)}\mathcal{P}_{11}(t,\mathcal{I}_\rho(t))\\
\quad+\frac{\alpha}{\mathcal{N}(\alpha)}\frac{1}{\Gamma(\alpha)}\int_0^t(t-\zeta)^{\alpha-1}\mathcal{P}_{11}(\zeta,\mathcal{I}_\rho(\zeta))d\zeta,\\
\mathcal{A}_\rho(t)-\mathcal{A}_\rho(0)=\frac{1-\alpha}{\mathcal{N}(\alpha)}\mathcal{P}_{12}(t,\mathcal{A}_\rho(t))\\
\quad+\frac{\alpha}{\mathcal{N}(\alpha)}\frac{1}{\Gamma(\alpha)}\int_0^t(t-\zeta)^{\alpha-1}\mathcal{P}_{12}(\zeta,\mathcal{A}_\rho(\zeta))d\zeta,\\
\mathcal{R}_\rho(t)-\mathcal{R}_\rho(0)=\frac{1-\alpha}{\mathcal{N}(\alpha)}\mathcal{P}_{13}(t,\mathcal{R}_\rho(t))\\
\quad+\frac{\alpha}{\mathcal{N}(\alpha)}\frac{1}{\Gamma(\alpha)}\int_0^t(t-\zeta)^{\alpha-1}\mathcal{P}_{13}(\zeta,\mathcal{R}_\rho(\zeta))d\zeta,\\
\mathcal{W}(t)-\mathcal{W}(0)=\frac{1-\alpha}{\mathcal{N}(\alpha)}\mathcal{P}_{14}(t,\mathcal{W}(t))\\
\quad+\frac{\alpha}{\mathcal{N}(\alpha)}\frac{1}{\Gamma(\alpha)}\int_0^t(t-\zeta)^{\alpha-1}\mathcal{P}_{14}(\zeta,\mathcal{W}(\zeta))d\zeta.
\end{cases}\tag{19}$$

To procure an iterative scheme, we go ahead with the first equation of the model (19) as follows:

$$\mathcal{S}_B(t)-\mathcal{S}_B(0)=\frac{1-\alpha}{\mathcal{N}(\alpha)}\mathcal{P}_1(t,\mathcal{S}_B(t))+\frac{\alpha}{\mathcal{N}(\alpha)}\frac{1}{\Gamma(\alpha)}\int_0^t(t-\zeta)^{\alpha-1}\mathcal{P}_1(\zeta,\mathcal{S}_B(\zeta))d\zeta,$$

Set $t=t_{r+1}$, for $r=0,1,2,\ldots$, it follows that

$$\begin{aligned}
\mathcal{S}_B(t_{r+1})-\mathcal{S}_B(0)&=\frac{1-\alpha}{\mathcal{N}(\alpha)}\mathcal{P}_1(t_r,\mathcal{S}_B(t_r))\\
&\quad+\frac{\alpha}{\mathcal{N}(\alpha)}\frac{1}{\Gamma(\alpha)}\int_0^{t_{r+1}}(t_{r+1}-\zeta)^{\alpha-1}\mathcal{P}_1(\zeta,\mathcal{S}_B(\zeta))d\zeta\\
&=\frac{1-\alpha}{\mathcal{N}(\alpha)}\mathcal{P}_1(t_r,\mathcal{S}_B(t_r))\\
&\quad+\frac{\alpha}{\mathcal{N}(\alpha)}\frac{1}{\Gamma(\alpha)}\\
&\quad\sum_{\ell=0}^{r}\int_{t_\ell}^{t_{\ell+1}}(t_{r+1}-\zeta)^{\alpha-1}\mathcal{P}_1(\zeta,\mathcal{S}_B(\zeta))d\zeta.
\end{aligned}\tag{20}$$

Now, we approximate the function $\mathcal{P}_1(\zeta,\mathcal{S}_B)$ on the interval $[t_\ell,t_{\ell+1}]$ through the interpolation polynomial as follows

$$\mathcal{P}_1(\zeta,\mathcal{S}_B(\zeta))\cong\frac{\mathcal{P}_1(t_\ell,\mathcal{S}_B(t_\ell))}{h}(t-t_{\ell-1})+\frac{\mathcal{P}_1(t_{\ell-1},\mathcal{S}_B(t_{\ell-1}))}{h}(t-t_\ell)$$

which implies

$$\begin{aligned}
\mathcal{S}_B(t_{r+1})&=\mathcal{S}_B(0)+\frac{1-\alpha}{\mathcal{N}(\alpha)}\mathcal{P}_1(t_r,\mathcal{S}_B(t_r))\\
&\quad+\frac{\alpha}{\mathcal{N}(\alpha)}\frac{1}{\Gamma(\alpha)}\\
&\quad\sum_{\ell=0}^{r}\left(\frac{\mathcal{P}_1(t_\ell,\mathcal{S}_B(t_\ell))}{h}\int_{t_\ell}^{t_{\ell+1}}(t-t_{\ell-1})(t_{r+1}-t)^{\alpha-1}dt\right.\\
&\quad\left.-\frac{\mathcal{P}_1(t_{\ell-1},\mathcal{S}_B(t_{\ell-1}))}{h}\int_{t_\ell}^{t_{\ell+1}}(t-t_\ell)(t_{r+1}-t)^{\alpha-1}dt\right)\\
&=\mathcal{S}_\rho(0)+\frac{1-\alpha}{\mathcal{N}(\alpha)}\mathcal{P}_1(t_r,\mathcal{S}_B(t_r))\\
&\quad+\frac{\alpha}{\mathcal{N}(\alpha)}\frac{1}{\Gamma(\alpha)}\\
&\quad\sum_{\ell=0}^{r}\left(\frac{\mathcal{P}_1(t_\ell,\mathcal{S}_B(t_\ell))}{h}I_{\ell-1,\alpha}-\frac{\mathcal{P}_1(t_{\ell-1},\mathcal{S}_B(t_{\ell-1}))}{h}I_{\ell,\alpha}\right),
\end{aligned}\tag{21}$$

Now, we compute the following integrals $I_{\ell-1,\alpha}$ and $I_{\ell,\alpha}$ as follws

$$\begin{aligned}
I_{\ell-1,\alpha}&=\int_{t_\ell}^{t_{\ell+1}}(t-t_{\ell-1})(t_{r+1}-t)^{\alpha-1}dt\\
&=-\frac{1}{\alpha}[(t_{\ell+1}-t_{\ell-1})(t_{r+1}-t_{\ell+1})^\alpha-(t_\ell-t_{\ell-1})(t_{r+1}-t_\ell)^\alpha]\\
&\quad-\frac{1}{\alpha(\alpha+1)}\left[(t_{r+1}-t_{\ell+1})^{\alpha+1}-(t_{r+1}-t_\ell)^{\alpha+1}\right],
\end{aligned}$$

and

$$\begin{aligned}
I_{\ell,\alpha}&=\int_{t_\ell}^{t_{\ell+1}}(t-t_\ell)(t_{r+1}-t)^{\alpha-1}dt\\
&=-\frac{1}{\alpha}[(t_{\ell+1}-t_\ell)(t_{r+1}-t_{\ell+1})^\alpha]\\
&\quad-\frac{1}{\alpha(\alpha+1)}\left[(t_{r+1}-t_{\ell+1})^{\alpha+1}-(t_{r+1}-t_\ell)^{\alpha+1}\right]
\end{aligned}$$

Put $t_\ell=\ell h$, we get

$$\begin{aligned}
I_{\ell-1,\alpha}&=-\frac{h^{\alpha+1}}{\alpha}[(\ell+1-(\ell-1))(r+1-(\ell+1))^\alpha\\
&\quad-(\ell-(\ell-1))(r+1-\ell)^\alpha]\\
&\quad-\frac{h^{\alpha+1}}{\alpha(\alpha+1)}\left[(r+1-(\ell+1))^{\alpha+1}-(r+1-\ell)^{\alpha+1}\right]\\
&=\frac{h^{\alpha+1}}{\alpha(\alpha+1)}[-2(\alpha+1)(r-\ell)^\alpha+(\alpha+1)(r+1-\ell)^\alpha\\
&\quad-(r-\ell)^{\alpha+1}+(r+1-\ell)^{\alpha+1}]\\
&=\frac{h^{\alpha+1}}{\alpha(\alpha+1)}[(r-\ell)^\alpha(-2(\alpha+1)-(r-\ell))\\
&\quad+(r+1-\ell)^\alpha(\alpha+1+r+1-\ell)]\\
&=\frac{h^{\alpha+1}}{\alpha(\alpha+1)}[(r+1-\ell)^\alpha(r-\ell+2+\alpha)\\
&\quad-(r-\ell)^\alpha(r-\ell+2+2\alpha)].
\end{aligned}\tag{22}$$

and

$$\begin{aligned}
I_{\ell,\alpha}&=-\frac{h^{\alpha+1}}{\alpha}[(\ell+1-\ell)(r+1-(\ell+1))^\alpha]\\
&\quad-\frac{h^{\alpha+1}}{\alpha(\alpha+1)}\left[(r+1-(\ell+1))^{\alpha+1}-(r+1-\ell)^{\alpha+1}\right]\\
&=\frac{h^{\alpha+1}}{\alpha(\alpha+1)}\left[-(\alpha+1)(r-\ell)^\alpha-(r-\ell)^{\alpha+1}+(r+1-\ell)^{\alpha+1}\right]\\
&=\frac{h^{\alpha+1}}{\alpha(\alpha+1)}\left[(r-\ell)^\alpha(-(\alpha+1)-(r-\ell))+(r+1-\ell)^{\alpha+1}\right]\\
&=\frac{h^{\alpha+1}}{\alpha(\alpha+1)}\left[(r+1-\ell)^{\alpha+1}-(r-\ell)^\alpha(r-\ell+1+\alpha)\right].
\end{aligned}\tag{23}$$

Substituting (22) and (23) into (21), we get

$$\mathcal{S}_B(t_{r+1})=\mathcal{S}_B(t_0)+\frac{1-\alpha}{\mathcal{N}(\alpha)}\mathcal{P}_1(t_r,\mathcal{S}_B(t_r))+\frac{\alpha}{\mathcal{N}(\alpha)}\sum_{\ell=0}^{r}$$

$$\left(\frac{\mathcal{P}_1(t_\ell,\mathcal{S}_B(t_\ell))}{\Gamma(\propto+2)}h^{\propto}[(r+1-\ell)^{\propto}(r-\ell+2+\propto)-(r-\ell)^{\propto}(r-\ell+2+2\propto)]-\frac{\mathcal{P}_1(t_{\ell-1},\mathcal{S}_B(t_{\ell-1}))}{\Gamma(\propto+2)}h^{\propto}\big[(r+1-\ell)^{\propto+1}-(r-\ell)^{\propto}(r-\ell+1+\propto)]\right). \tag{24}$$

Similarly

$$\mathcal{E}_B(t_{r+1})=\mathcal{E}_B(t_0)+\frac{1-\propto}{\mathcal{N}(\propto)}\mathcal{P}_2(t_r,\mathcal{E}_B(t_r))+\frac{\propto}{\mathcal{N}(\propto)}\sum_{\ell=0}^{r}\left(\frac{\mathcal{P}_2(t_\ell,\mathcal{E}_B(t_\ell))}{\Gamma(\propto+2)}h^{\propto}[(r+1-\ell)^{\propto}(r-\ell+2+\propto)-(r-\ell)^{\propto}(r-\ell+2+2\propto)]-\frac{\mathcal{P}_2(t_{\ell-1},\mathcal{E}_B(t_{\ell-1}))}{\Gamma(\propto+2)}h^{\propto}\big[(r+1-\ell)^{\propto+1}-(r-\ell)^{\propto}(r-\ell+1+\propto)]\right), \tag{25}$$

$$\mathcal{I}_B(t_{r+1})=\mathcal{I}_B(t_0)+\frac{1-\propto}{\mathcal{N}(\propto)}\mathcal{P}_3(t_r,\mathcal{I}_B(t_r))+\frac{\propto}{\mathcal{N}(\propto)}\sum_{\ell=0}^{r}\left(\frac{\mathcal{P}_3(t_\ell,\mathcal{I}_B(t_\ell))}{\Gamma(\propto+2)}h^{\propto}[(r+1-\ell)^{\propto}(r-\ell+2+\propto)-(r-\ell)^{\propto}(r-\ell+2+2\propto)]-\frac{\mathcal{P}_3(t_{\ell-1},\mathcal{I}_B(t_{\ell-1}))}{\Gamma(\propto+2)}h^{\propto}\big[(r+1-\ell)^{\propto+1}-(r-\ell)^{\propto}(r-\ell+1+\propto)]\right), \tag{26}$$

$$\mathcal{R}_B(t_{r+1})=\mathcal{R}_B(t_0)+\frac{1-\propto}{\mathcal{N}(\propto)}\mathcal{P}_4(t_r,\mathcal{R}_B(t_r))+\frac{\propto}{\mathcal{N}(\propto)}\sum_{\ell=0}^{r}\left(\frac{\mathcal{P}_4(t_\ell,\mathcal{R}_B(t_\ell))}{\Gamma(\propto+2)}h^{\propto}[(r+1-\ell)^{\propto}(r-\ell+2+\propto)-(r-\ell)^{\propto}(r-\ell+2+2\propto)]-\frac{\mathcal{P}_4(t_{\ell-1},\mathcal{R}_B(t_{\ell-1}))}{\Gamma(\propto+2)}h^{\propto}\big[(r+1-\ell)^{\propto+1}-(r-\ell)^{\propto}(r-\ell+1+\propto)]\right), \tag{27}$$

$$\mathcal{S}_H(t_{r+1})=\mathcal{S}_H(t_0)+\frac{1-\propto}{\mathcal{N}(\propto)}\mathcal{P}_1(t_r,\mathcal{S}_H(t_r))+\frac{\propto}{\mathcal{N}(\propto)}\sum_{\ell=0}^{r}\left(\frac{\mathcal{P}_1(t_\ell,\mathcal{S}_H(t_\ell))}{\Gamma(\propto+2)}h^{\propto}[(r+1-\ell)^{\propto}(r-\ell+2+\propto)-(r-\ell)^{\propto}(r-\ell+2+2\propto)]-\frac{\mathcal{P}_1(t_{\ell-1},\mathcal{S}_H(t_{\ell-1}))}{\Gamma(\propto+2)}h^{\propto}\big[(r+1-\ell)^{\propto+1}-(r-\ell)^{\propto}(r-\ell+1+\propto)]\right), \tag{28}$$

$$\mathcal{E}_H(t_{r+1})=\mathcal{E}_H(t_0)+\frac{1-\propto}{\mathcal{N}(\propto)}\mathcal{P}_2(t_r,\mathcal{E}_H(t_r))+\frac{\propto}{\mathcal{N}(\propto)}\sum_{\ell=0}^{r}\left(\frac{\mathcal{P}_2(t_\ell,\mathcal{E}_H(t_\ell))}{\Gamma(\propto+2)}h^{\propto}[(r+1-\ell)^{\propto}(r-\ell+2+\propto)-(r-\ell)^{\propto}(r-\ell+2+2\propto)]-\frac{\mathcal{P}_2(t_{\ell-1},\mathcal{E}_H(t_{\ell-1}))}{\Gamma(\propto+2)}h^{\propto}\big[(r+1-\ell)^{\propto+1}-(r-\ell)^{\propto}(r-\ell+1+\propto)]\right), \tag{29}$$

$$\mathcal{I}_H(t_{r+1})=\mathcal{I}_H(t_0)+\frac{1-\propto}{\mathcal{N}(\propto)}\mathcal{P}_3(t_r,\mathcal{I}_H(t_r))+\frac{\propto}{\mathcal{N}(\propto)}\sum_{\ell=0}^{r}\left(\frac{\mathcal{P}_3(t_\ell,\mathcal{I}_H(t_\ell))}{\Gamma(\propto+2)}h^{\propto}[(r+1-\ell)^{\propto}(r-\ell+2+\propto)-(r-\ell)^{\propto}(r-\ell+2+2\propto)]-\frac{\mathcal{P}_3(t_{\ell-1},\mathcal{I}_H(t_{\ell-1}))}{\Gamma(\propto+2)}h^{\propto}\big[(r+1-\ell)^{\propto+1}-(r-\ell)^{\propto}(r-\ell+1+\propto)]\right), \tag{30}$$

$$\mathcal{R}_H(t_{r+1})=\mathcal{R}_H(t_0)+\frac{1-\propto}{\mathcal{N}(\propto)}\mathcal{P}_4(t_r,\mathcal{R}_H(t_r))+\frac{\propto}{\mathcal{N}(\propto)}\sum_{\ell=0}^{r}\left(\frac{\mathcal{P}_4(t_\ell,\mathcal{R}_H(t_\ell))}{\Gamma(\propto+2)}h^{\propto}[(r+1-\ell)^{\propto}(r-\ell+2+\propto)-(r-\ell)^{\propto}(r-\ell+2+2\propto)]-\frac{\mathcal{P}_4(t_{\ell-1},\mathcal{R}_H(t_{\ell-1}))}{\Gamma(\propto+2)}h^{\propto}\big[(r+1-\ell)^{\propto+1}-(r-\ell)^{\propto}(r-\ell+1+\propto)]\right), \tag{31}$$

$$\mathcal{S}_\rho(t_{r+1})=\mathcal{S}_\rho(t_0)+\frac{1-\propto}{\mathcal{N}(\propto)}\mathcal{P}_1(t_r,\mathcal{S}_\rho(t_r))+\frac{\propto}{\mathcal{N}(\propto)}\sum_{\ell=0}^{r}\left(\frac{\mathcal{P}_1(t_\ell,\mathcal{S}_\rho(t_\ell))}{\Gamma(\propto+2)}h^{\propto}[(r+1-\ell)^{\propto}(r-\ell+2+\propto)-(r-\ell)^{\propto}(r-\ell+2+2\propto)]-\frac{\mathcal{P}_1(t_{\ell-1},\mathcal{S}_\rho(t_{\ell-1}))}{\Gamma(\propto+2)}h^{\propto}\big[(r+1-\ell)^{\propto+1}-(r-\ell)^{\propto}(r-\ell+1+\propto)]\right), \tag{32}$$

$$\mathcal{E}_\rho(t_{r+1})=\mathcal{E}_\rho(t_0)+\frac{1-\propto}{\mathcal{N}(\propto)}\mathcal{P}_2(t_r,\mathcal{E}_\rho(t_r))+\frac{\propto}{\mathcal{N}(\propto)}\sum_{\ell=0}^{r}\left(\frac{\mathcal{P}_2(t_\ell,\mathcal{E}_\rho(t_\ell))}{\Gamma(\propto+2)}h^{\propto}[(r+1-\ell)^{\propto}(r-\ell+2+\propto)-(r-\ell)^{\propto}(r-\ell+2+2\propto)]-\frac{\mathcal{P}_2(t_{\ell-1},\mathcal{E}_\rho(t_{\ell-1}))}{\Gamma(\propto+2)}h^{\propto}\big[(r+1-\ell)^{\propto+1}-(r-\ell)^{\propto}(r-\ell+1+\propto)]\right), \tag{33}$$

$$\mathcal{I}_\rho(t_{r+1})=\mathcal{I}_\rho(t_0)+\frac{1-\propto}{\mathcal{N}(\propto)}\mathcal{P}_3(t_r,\mathcal{I}_\rho(t_r))+\frac{\propto}{\mathcal{N}(\propto)}\sum_{\ell=0}^{r}\left(\frac{\mathcal{P}_3(t_\ell,\mathcal{I}_\rho(t_\ell))}{\Gamma(\propto+2)}h^{\propto}[(r+1-\ell)^{\propto}(r-\ell+2+\propto)-(r-\ell)^{\propto}(r-\ell+2+2\propto)]-\frac{\mathcal{P}_3(t_{\ell-1},\mathcal{I}_\rho(t_{\ell-1}))}{\Gamma(\propto+2)}h^{\propto}\big[(r+1-\ell)^{\propto+1}-(r-\ell)^{\propto}(r-\ell+1+\propto)]\right), \tag{34}$$

Table 1
Numerical values and the physical interpretation of the parameters involve in the proposed model (1).

Parameters	physical description	Numerical value
Λ_B	The birth rate parameter of bats	0.0300
m_B	The death rate of bats	0.011
β_B	The transmission rate from $\mathcal{I}_B$ to $\mathcal{S}_B$	0.01166
$\frac{1}{\omega_B}$	The incubation period of bats	0.00073
$\frac{1}{\gamma_B}$	The infectious period of bats	0.0345
Λ_H	Recruitment from total number of hosts	1*millions*
m_H	The death rate of hosts	0.011
β_H	The transmission rate from $\mathcal{I}_H$ to $\mathcal{S}_H$	0.0300
β_{BH}	The transmission rate from $\mathcal{I}_B$ to $\mathcal{S}_H$	0.0405
Λ_ρ	The birth rate parameter of people	1.00
m_ρ	The death rate of people	0.0091
β_ρ	The transmission rate from $\mathcal{I}_p$ to $\mathcal{S}_p$	0.004
κ	The multiple of the transmissibility of $\mathcal{A}_p$ to $\mathcal{I}_p$	0.003
β_ω	The transmission rate from $\mathcal{W}$ to $\mathcal{S}_p$	0.005
β_ρ	The transmission rate from $\mathcal{I}_p$ to $\mathcal{S}_p$	0.001
δ_ρ	The proportion of asymptomatic infection rate of people	0.002
$\frac{1}{\omega_\rho'}$	The latent period of people	0.003
γ_ρ	The infectious period of symptomatic infection of people	0.005
a	The retail purchases rate of the hosts in the market	0.0321
$\frac{1}{\gamma_\rho'}$	The infectious period of asymptomatic infection of people	0.0121
μ	The shedding coefficients from $\mathcal{I}_\rho$ to $\mathcal{W}$	0.0121
μ_ρ'	The shedding coefficients from $\mathcal{A}_\rho$ to $\mathcal{W}$	0.0761
$\frac{1}{\varepsilon}$	The lifetime of the virus in $\mathcal{W}$	0.0261
$\mathcal{N}_H$	The total number of hosts	10 millions

$$\mathcal{A}_\rho(t_{r+1}) = \mathcal{A}_\rho(t_0) + \frac{1-\propto}{\mathcal{N}(\propto)}\mathcal{P}_4(t_r, \mathcal{A}_\rho(t_r)) + \frac{\propto}{\mathcal{N}(\propto)}\sum_{\ell=0}^{r}$$
$$\left(\frac{\mathcal{P}_4(t_\ell, \mathcal{A}_\rho(t_\ell))}{\Gamma(\propto+2)}h^\propto[(r+1-\ell)^\propto(r-\ell+2+\propto)\right.$$
$$-(r-\ell)^\propto(r-\ell+2+2\propto)]$$
$$-\frac{\mathcal{P}_4(t_{\ell-1}, \mathcal{A}_\rho(t_{\ell-1}))}{\Gamma(\propto+2)}h^\propto\big[(r+1-\ell)^{\propto+1}$$
$$\left.-(r-\ell)^\propto(r-\ell+1+\propto)]\right), \tag{35}$$

$$\mathcal{R}_\rho(t_{r+1}) = \mathcal{R}_\rho(t_0) + \frac{1-\propto}{\mathcal{N}(\propto)}\mathcal{P}_5(t_r, \mathcal{R}_\rho(t_r)) + \frac{\propto}{\mathcal{N}(\propto)}\sum_{\ell=0}^{r}$$
$$\left(\frac{\mathcal{P}_5(t_\ell, \mathcal{R}_\rho(t_\ell))}{\Gamma(\propto+2)}h^\propto[(r+1-\ell)^\propto(r-\ell+2+\propto)\right.$$
$$-(r-\ell)^\propto(r-\ell+2+2\propto)]$$
$$-\frac{\mathcal{P}_5(t_{\ell-1}, \mathcal{R}_\rho(t_{\ell-1}))}{\Gamma(\propto+2)}h^\propto\big[(r+1-\ell)^{\propto+1}$$
$$\left.-(r-\ell)^\propto(r-\ell+1+\propto)]\right). \tag{36}$$

$$\mathcal{W}(t_{r+1}) = \mathcal{W}(t_0) + \frac{1-\propto}{\mathcal{N}(\propto)}\mathcal{P}_6(t_r, \mathcal{W}(t_r)) + \frac{\propto}{\mathcal{N}(\propto)}\sum_{\ell=0}^{r}$$
$$\left(\frac{\mathcal{P}_6(t_\ell, \mathcal{W}(t_\ell))}{\Gamma(\propto+2)}h^\propto[(r+1-\ell)^\propto(r-\ell+2+\propto)\right.$$
$$-(r-\ell)^\propto(r-\ell+2+2\propto)]$$
$$-\frac{\mathcal{P}_6(t_{\ell-1}, \mathcal{W}(t_{\ell-1}))}{\Gamma(\propto+2)}h^\propto\big[(r+1-\ell)^{\propto+1}$$
$$\left.-(r-\ell)^\propto(r-\ell+1+\propto)]\right). \tag{37}$$

5.1. Numerical interpretation and discussion

Now to present the numerical simulations of the ABC fractional model (1)-(2), we apply the iterative solution contained in (24)-(37). Taking the time in (Days) . The numerical amounts of the parameters applied in the simulations are specified in Table 1. The graphical representations of numerical solution for species $\mathcal{S}_B, \mathcal{E}_B, \mathcal{I}_B, \mathcal{R}_B, \mathcal{S}_H, \mathcal{E}_H, \mathcal{I}_H, \mathcal{R}_H, \mathcal{S}_\rho, \mathcal{E}_\rho, \mathcal{I}_\rho, \mathcal{A}_\rho, \mathcal{R}_\rho, \mathcal{W}$ at various fractional-order $\propto = 0.4, 0.6, 0.8, 1.0$ of the considered model (1) are given in Figs. 1, 2, 3, 4, 5, 6, 7, 8, 9, 10, 11, 12, 13, 14 respectively. We simulate the results for first hundred days and hence our interval of study in numerical simulation is $J = [0, 100]$. We take initial values in percentage of the total papulation as

$$\mathcal{S}_B(0) = 0.6,\ \mathcal{E}_B(0) = 0.2,\ \mathcal{I}_B(0) = 0.1,$$
$$\mathcal{R}_B(0) = 0,\ \mathcal{S}_H(0) = 0.03,\ \mathcal{E}_H(0) = .01,$$
$$\mathcal{I}_H(0) = 0.03,\ \mathcal{R}_H(0) = 0.001,\ \mathcal{S}_\rho(0) = 0.01,$$
$$\mathcal{E}_\rho(0) = 0.003,\ \mathcal{I}_\rho(0) = 0.9,$$
$$\mathcal{A}_\rho(0) = 0.001,\ \mathcal{R}_\rho(0) = 0,\ \mathcal{W}(0) = 0.$$

In Figs. 1–14, we have given a global dynamics of each compartment in the considered model (1) by using the numerical values in Table 1 against different fractional order. The growth and decay of various compartment is different that some compartments are growing with different rate due to fractional order and similar behavior may be observed for decay of some compartments. Lower the order faster is the growing rate and vice versa and similarly the decay also is different at different fractional order. Therefore fractional calculus can help in understanding the transmission dynamics of novel coronavirus-19 disease. Also the concerned numerical scheme can be used as a powerful tools to perform numerical simulation of such complicated model. In Fig. 1 as susceptible papulation is decreasing as they are exposing so the density of expose class is going on growing as in Fig. 2. On the other hand the infected bats density is increasing as presented in Fig. 3, while the number of removed bats are also increasing in Fig. 4 until stable in the market. On the other hand as the density of susceptible host is decreasing in Fig. 5 because they are exposing to infection. Therefore the density of exposed host is growing as in Fig. 6 as a results

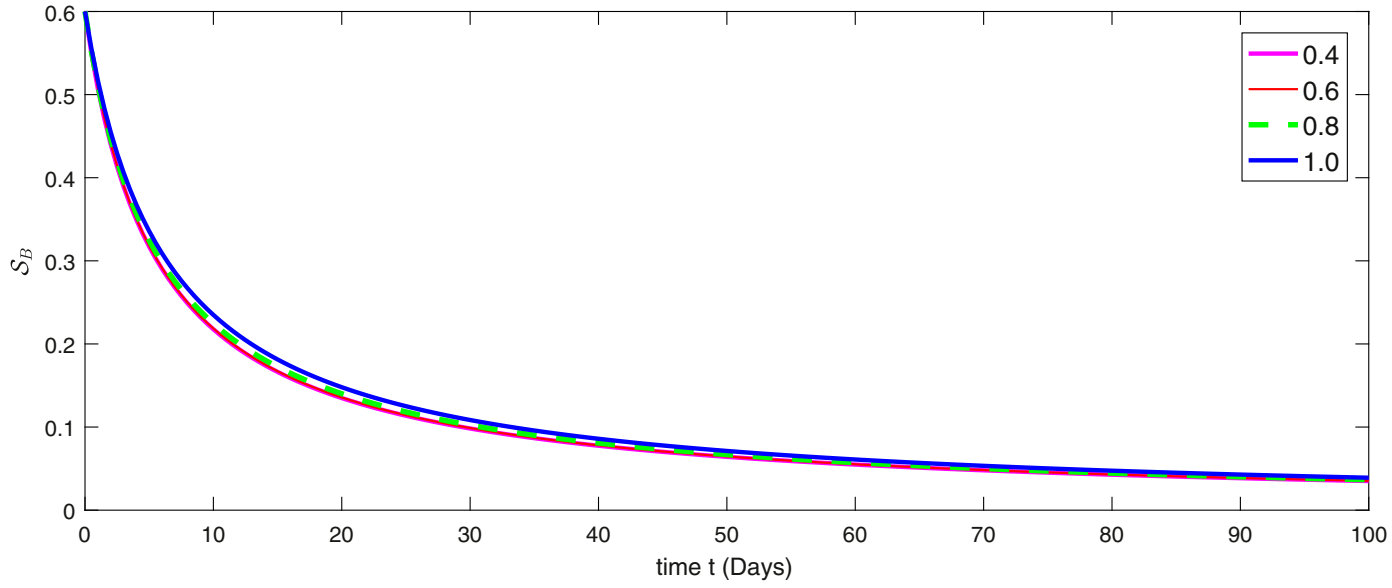

Fig. 1. Graphical representation of numerical solution for susceptible class of bats at various fractional of the considered model (1).

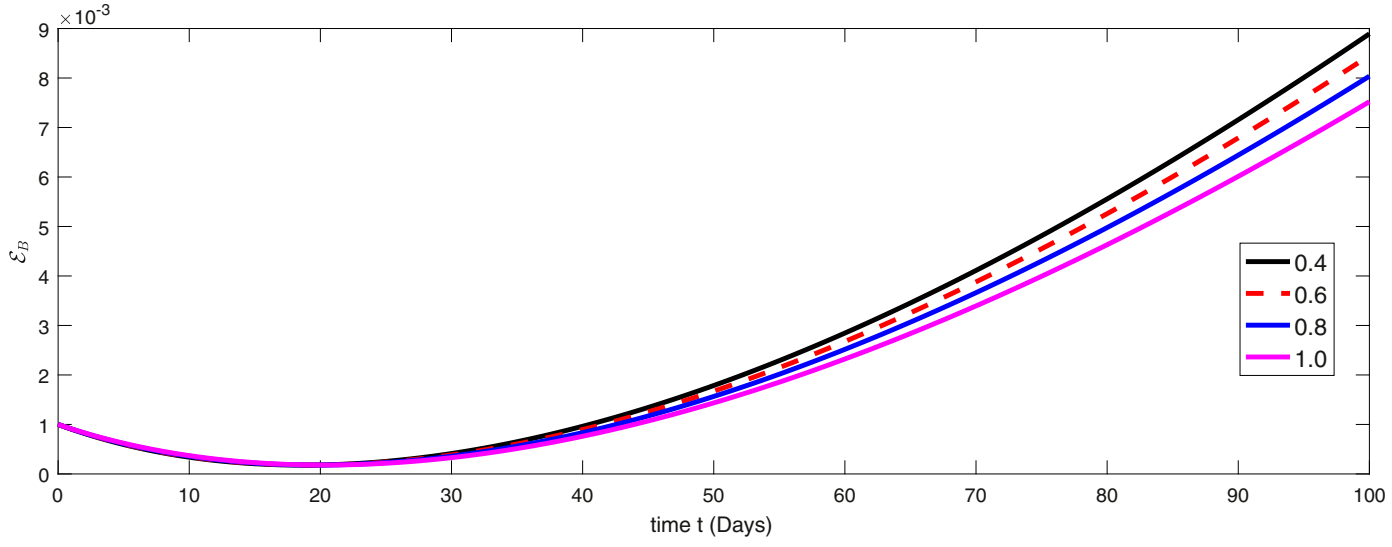

Fig. 2. Graphical representation of numerical solution for exposed bats at various fractional of the considered model (1).

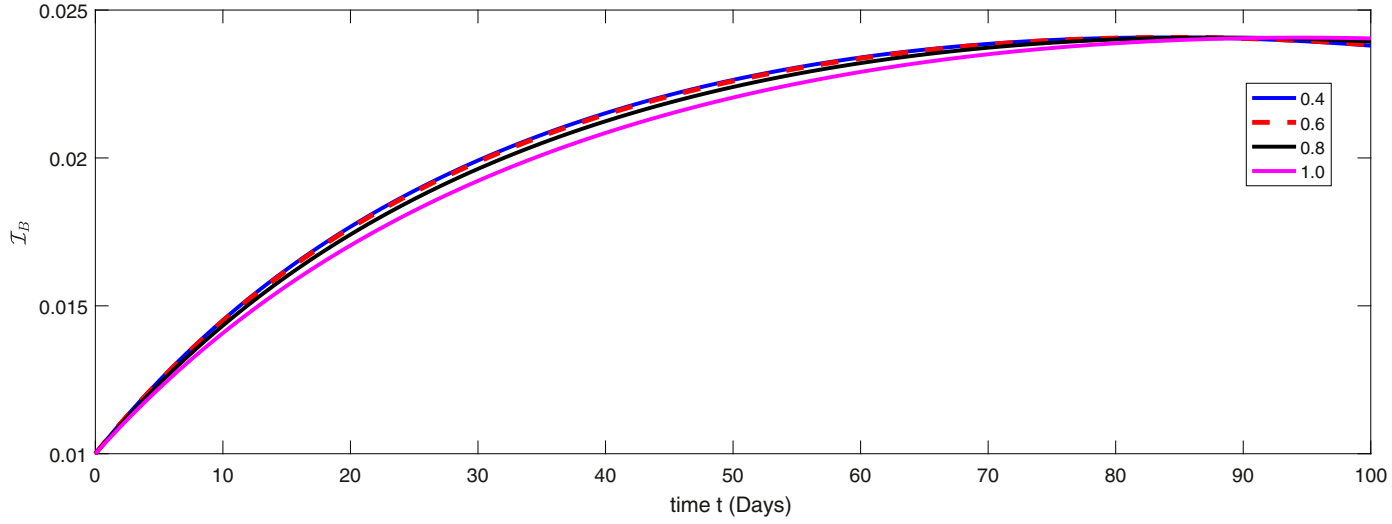

Fig. 3. Graphical representation of numerical solution for infected bats at various fractional of the considered model (1).

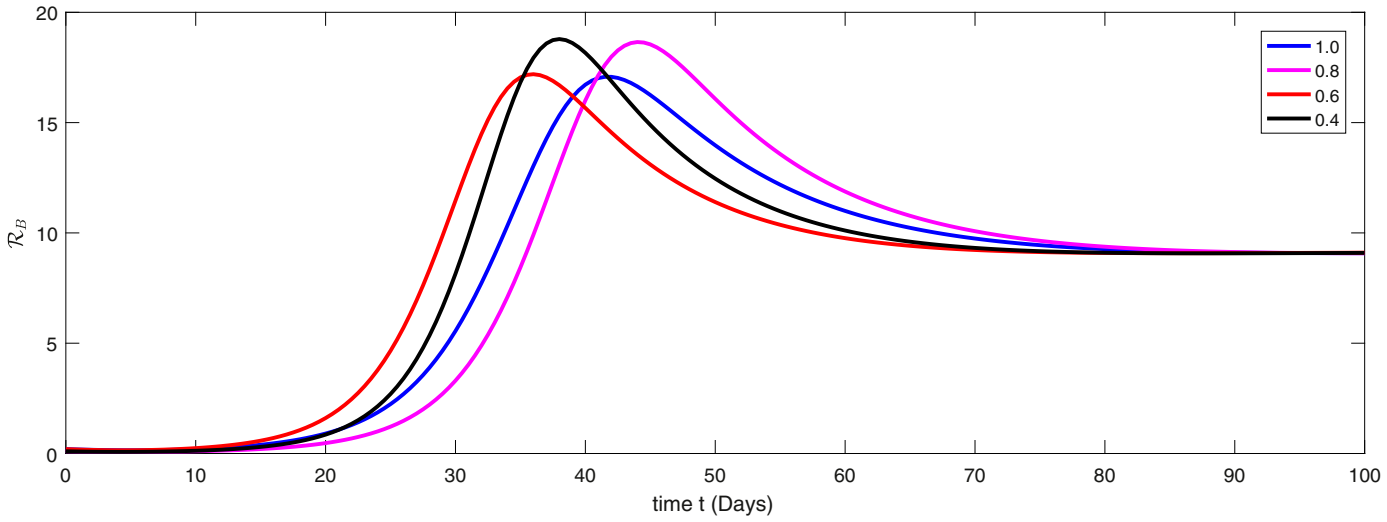

Fig. 4. Graphical representation of numerical solution for removed class of bats at various fractional of the considered model (1).

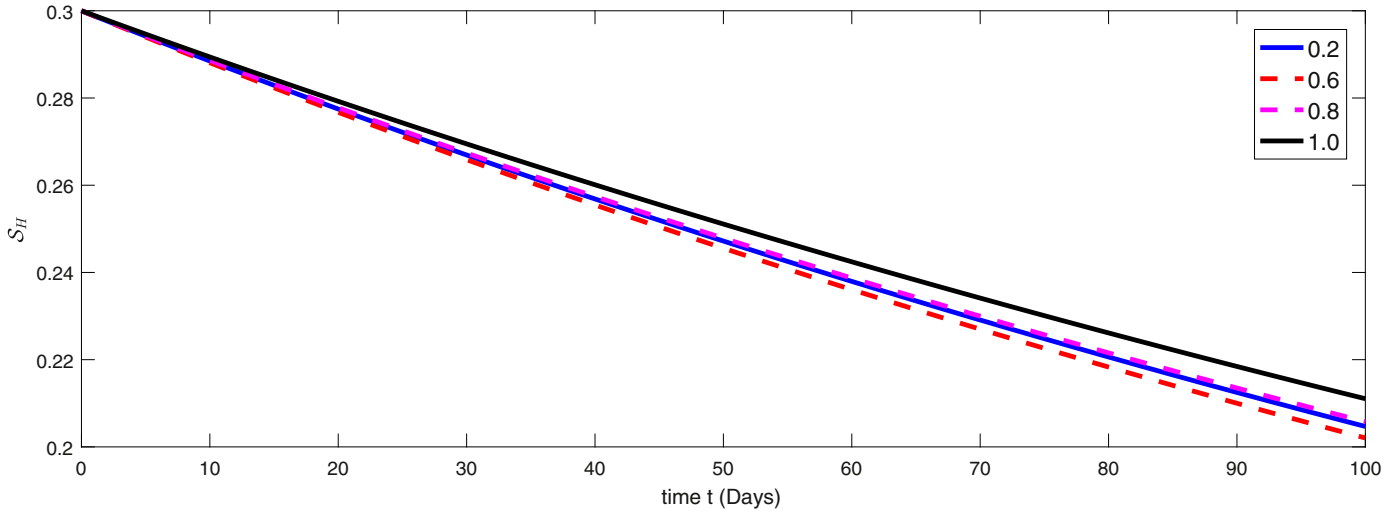

Fig. 5. Graphical representation of numerical solution for susceptible host at various fractional of the considered model (1).

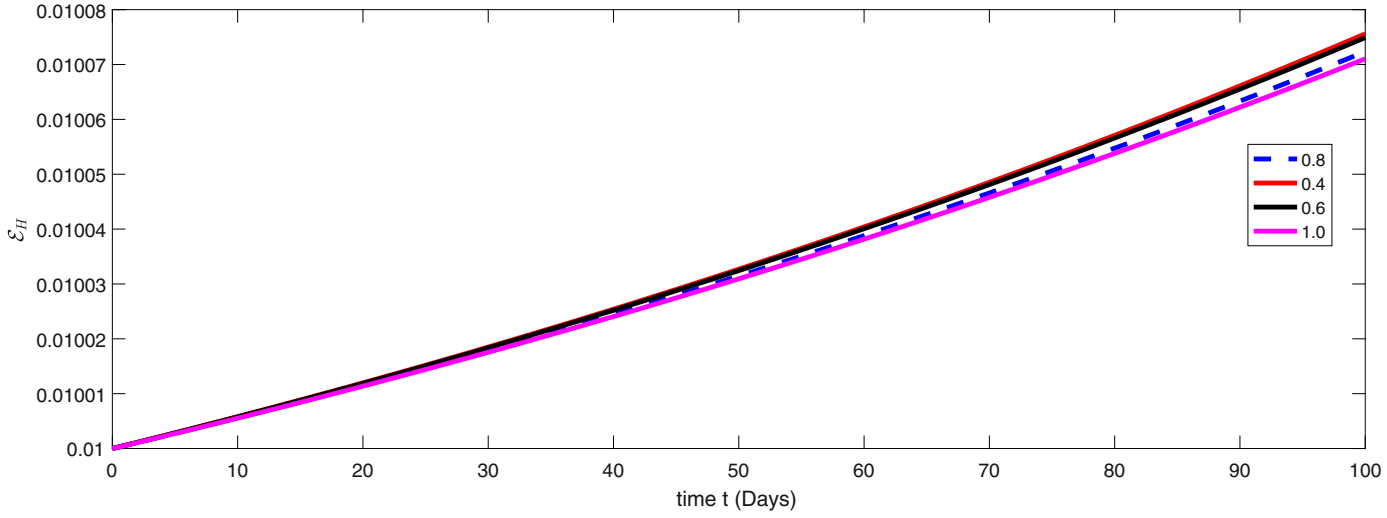

Fig. 6. Graphical representation of numerical solution for exposed hosts at various fractional of the considered model (1).

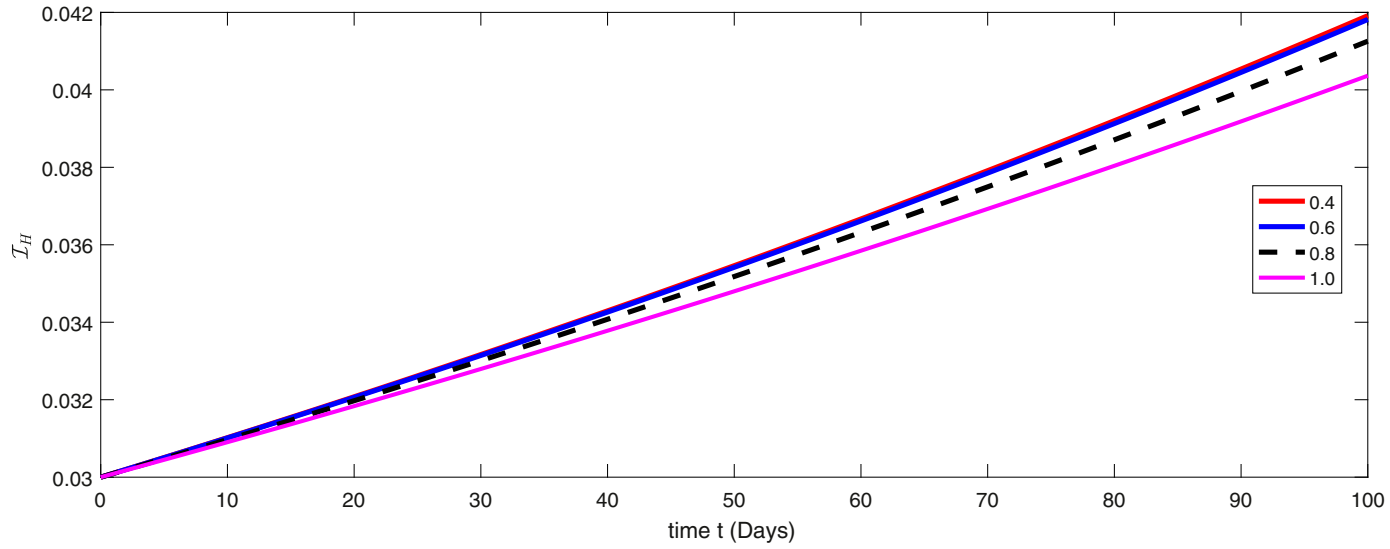

Fig. 7. Graphical representation of numerical solution for infected host at various fractional of the considered model (1).

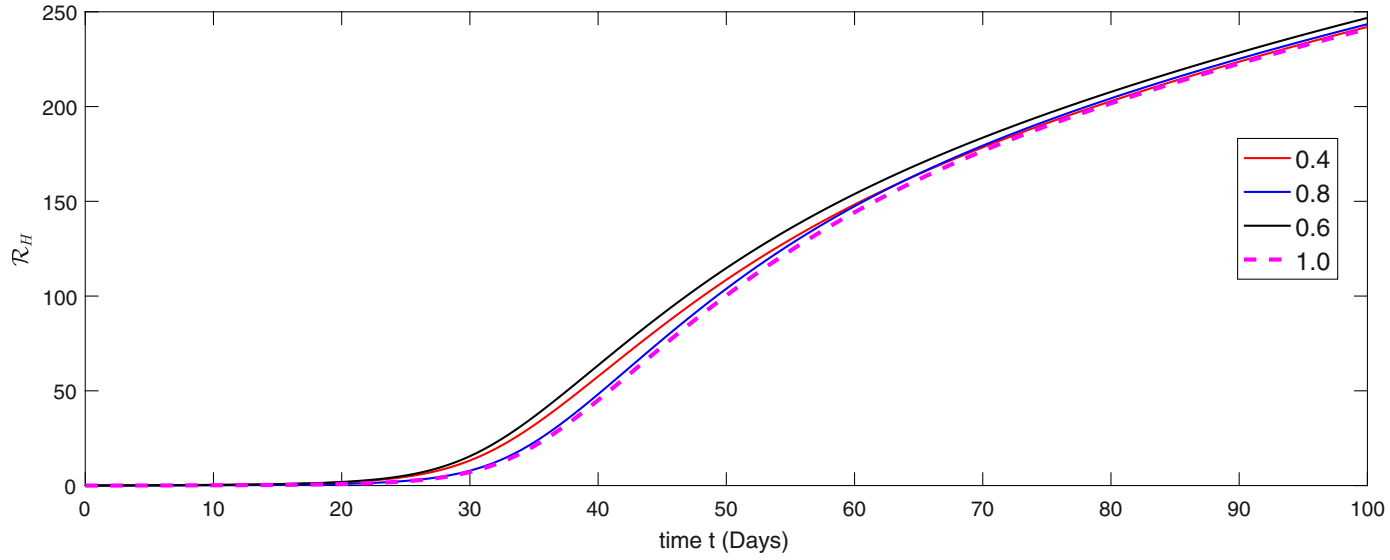

Fig. 8. Graphical representation of numerical solution for removed host at various fractional of the considered model (1).

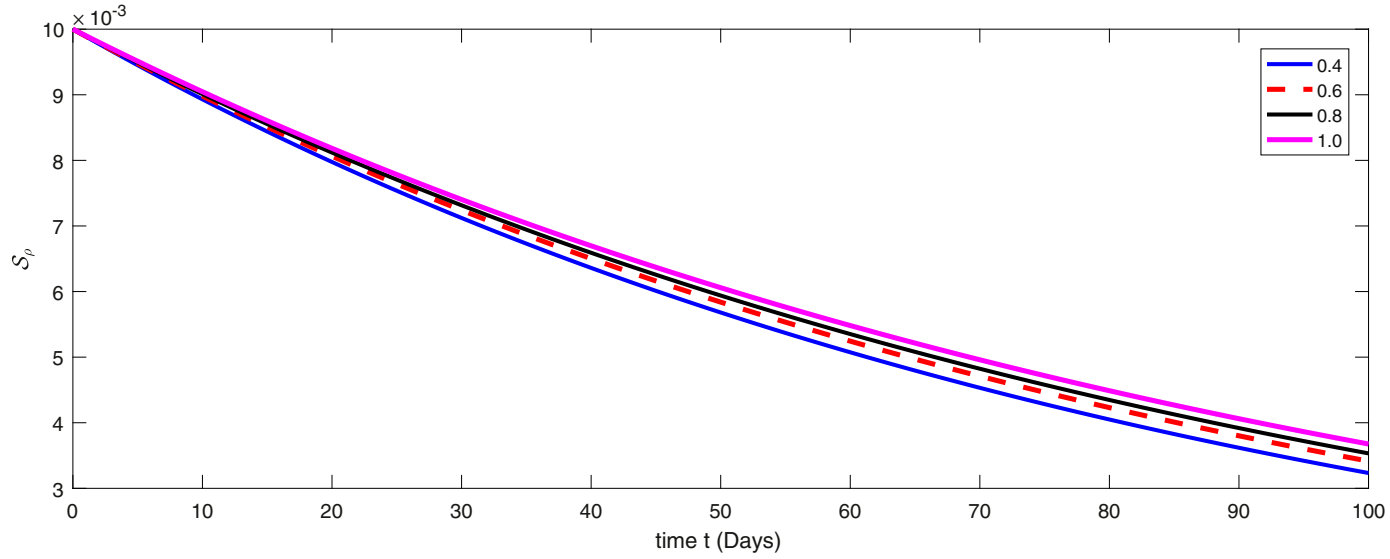

Fig. 9. Graphical representation of numerical solution for susceptible people at various fractional of the considered model (1).

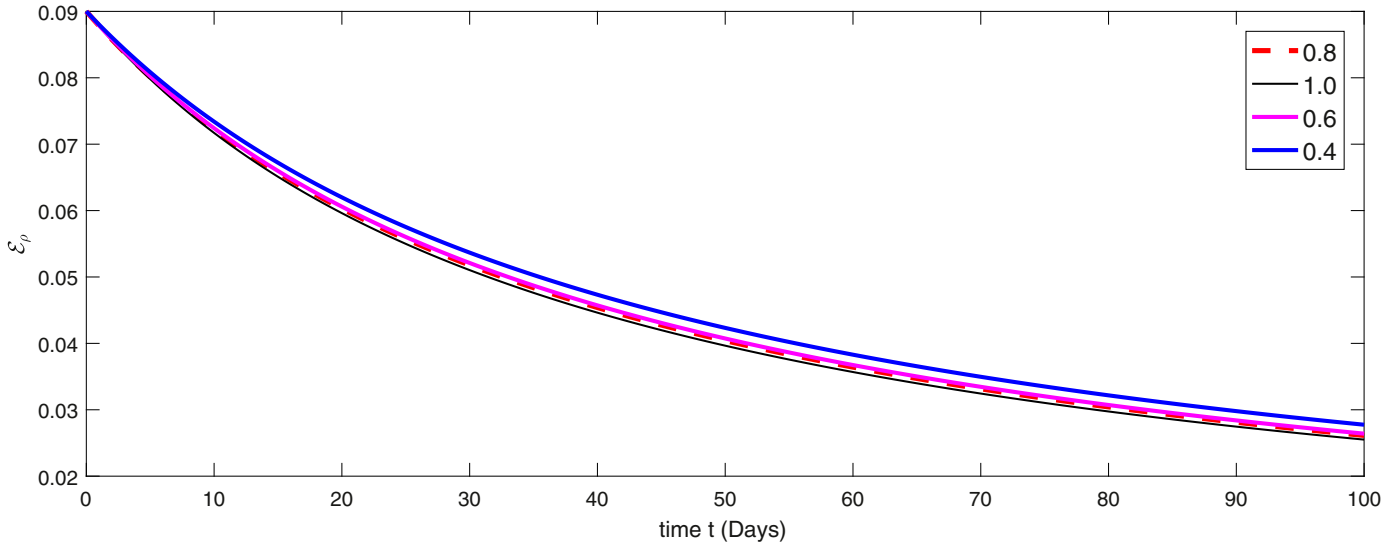

Fig. 10. Graphical representation of numerical solution for exposed people at various fractional of the considered model (1).

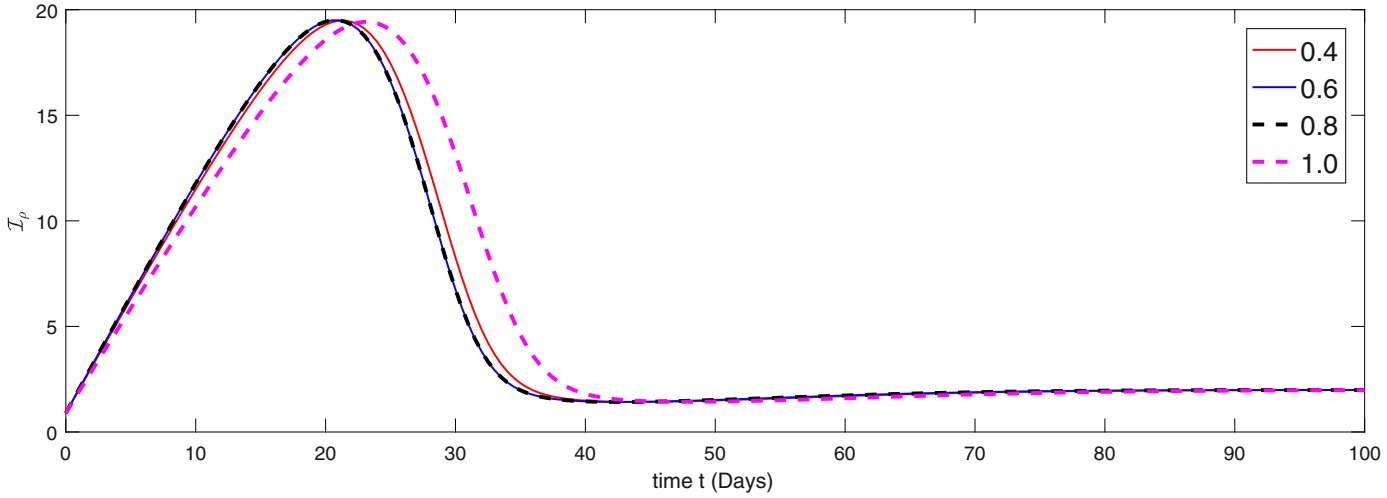

Fig. 11. Graphical representation of numerical solution for symptomatic infected people at various fractional of the considered model (1).

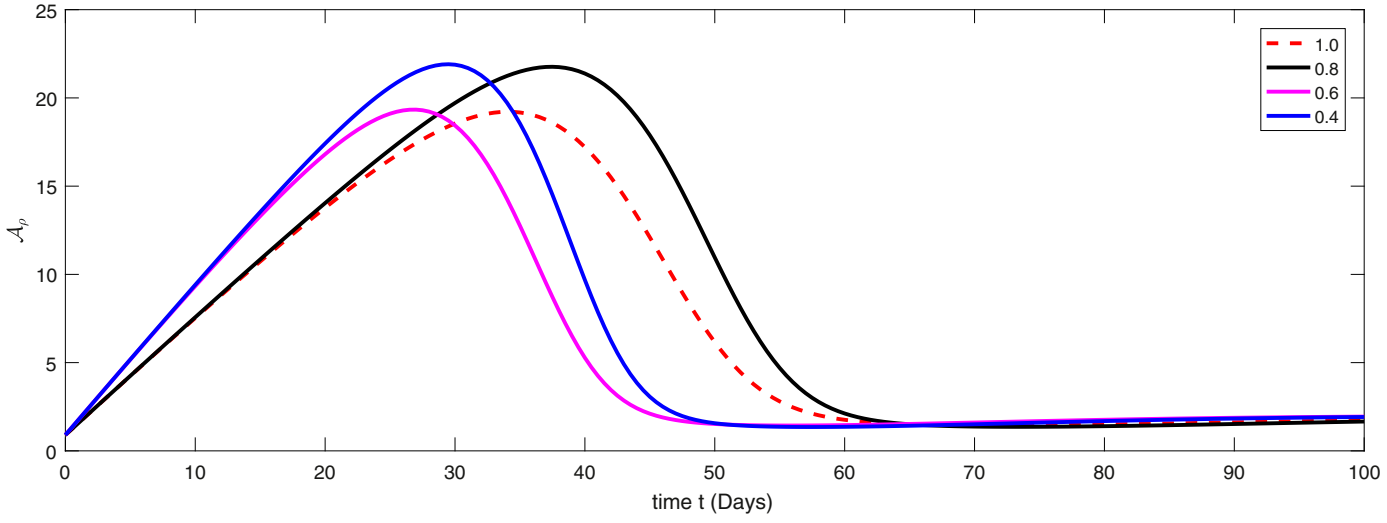

Fig. 12. Graphical representation of numerical solution for asymptomatic infected people at various fractional of the considered model (1).

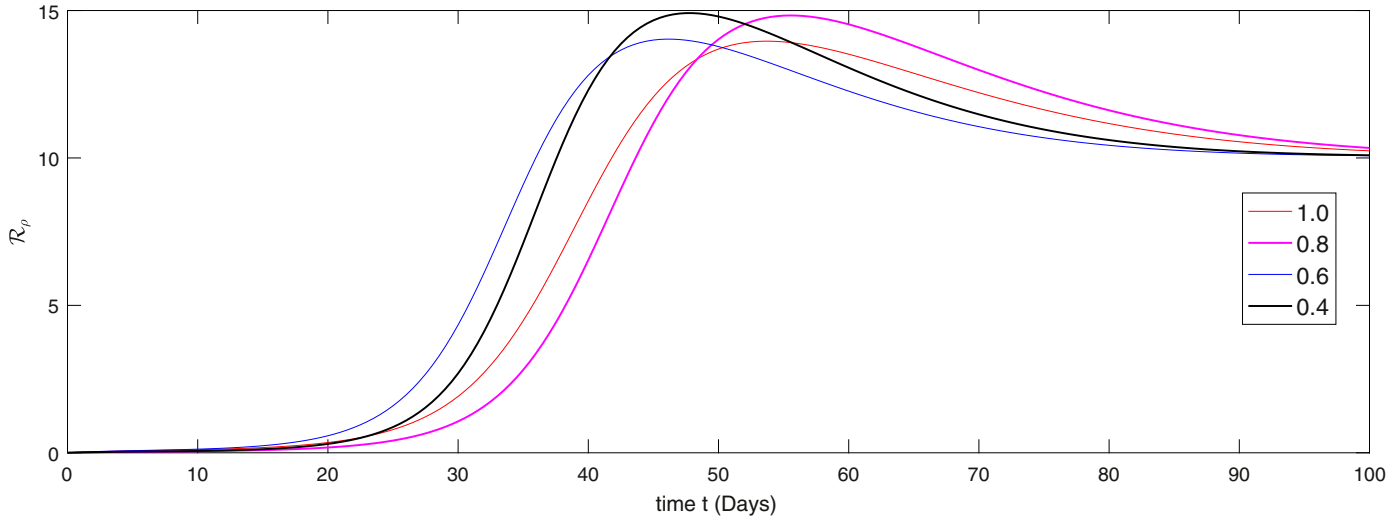

Fig. 13. Graphical representation of numerical solution for population of removed people due to death or recovered various fractional of the considered model (1).

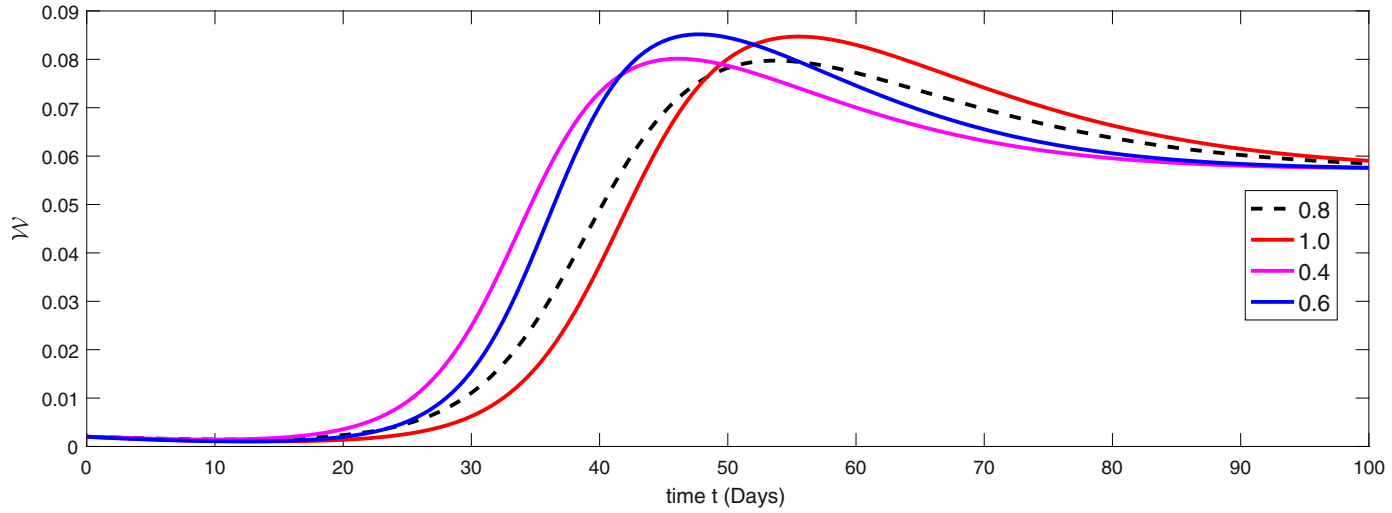

Fig. 14. Graphical representation of numerical solution for population of virus in reservoir various fractional of the considered model (1).

the host catching more infecting and hence the density of host infected is also increasing. This process may be observed from Fig. 7. As a results of infection the removed (either death or get ride from infection) will increasing as in Fig. 8. In same way the density of susceptible people is decreasing in Fig. 9 because they are exposing to infection so the density of exposed people will decrease (see Fig. 10), because the people rapidly catching infection, hence the density of symptomatic infected people will grow as in Fig. 11. The similar behavior one can observed for density of asymptomatic and removed (either death or recovered from infection) in Figs. 12 and 13 respectively. Since as the density of infected bats is increasing, also the infection in host papulation is growing. As a result the papulation of virus in reservoir will grow further as presented in Fig. 14.

6. Conclusion

This manuscript has been devoted to comprehensively investigate a mathematical model for calculating the transmissibility of novel Coronavirus (COVID-19) disease by using nonsingular fractional order derivative. The existence and uniqueness of the considered model has been guaranteed by applying Krasnoselskii and Banach fixed point theorems. Also some stability results of Ulam type have been constructed. With the help of fractional Adams Bashforth method method we have simulated the results corresponding to various fractional orders. The obtained results play important role in developing the theory of fractional analytical dynamic for the current pandemic due to Coronavirus -19 which has badly affected the whole world. From the simulation we noted that the decrease in susceptibility is faster at lower fractional order of the derivative and in same line the increase in infections is also rapid with smaller order. The presented results may be helpful in understanding the present pandemic more comprehensively and can help in taking precautionary measure to reduce the infection to minimum.

Declaration of Competing Interest

We declare that none of the author has the competing or conflict of interest.

CRediT authorship contribution statement

Mohammed S. Abdo: Writing - original draft. **Kamal Shah:** Methodology. **Hanan A. Wahash:** Formal analysis. **Satish K. Panchal:** Writing - review & editing.

Acknowledgment

We are thankful to the reviewers for their constructive suggestions which improved this paper very well.

References

[1] Lu H, Stratton CW, Tang YW. Outbreak of pneumonia of unknown etiology in Wuhan China: the mystery and the miracle. J Med Virol 2020. doi:10.1002/jmv.25678.
[2] Ji W, Wang W, Zhao X, Zai J, Li X. Homologous recombination within the spike glycoprotein of the newly identified coronavirus may boost cross-species transmission from snake to human. J Med Virol 2020. doi:10.1002/jmv.25682.
[3] Tyrrell DA, Bynoe ML. Cultivation of viruses from a high proportion of patients with colds. Lancet 1966;1:76–7.
[4] Kahn JS, McIntosh K. History and recent advances in coronavirus discovery. Pediatric Infect Dis J 2005;24(11):223–7.
[5] Kilbas AA, Shrivastava HM, Trujillo JJ. Theory and applications of fractional differential equations. Amsterdam: Elsevier; 2006.
[6] Podlubny I. Fractionaldifferential equations. San Diego: Academic; 1999.
[7] Caputo M, Fabrizio M. A new definition of fractional derivative without singular kernel. Prog Fract Differ Appl 2015;1(2):73–85.
[8] Atangana A, Baleanu D. New fractional derivatives with non-local and non-singular kernel: theory and application to heat transfer model. Therm Sci 2016;20(2):763–9.
[9] Atangana A. Non validity of index law in fractional calculus: a fractional differential operator with Markovian and non-Markovian properties. Phys A Stat Mech Appl 2018;505:688–706.
[10] Atangana A, Gómez-Aguilar JF. Fractional derivatives with no-index law property: application to chaos and statistics. Chaos Soliton Fract 2018;114:516–35.
[11] Atangana A, Gómez-Aguilar JF. Decolonisation of fractional calculus rules: breaking commutativity and associativity to capture more natural phenomena. Eur Phys J Plus 2018;133:1–22.
[12] Chen T, Rui J, Wang Q, Zhao Z, Cui J, Yin L. A mathematical model for simulating the phase-based transmissibility of a novel coronavirus. Infect Dis Poverty 2020;9(24).
[13] Azhar H., Dumitru B., Saman Y.. On a nonlinear fractional-order model of novel coronavirus (NCOV-2019) under AB-fractional derivative. To appear2020;.
[14] Lin Q, Zhao S, Gao D, Lou Y, Yang S, Musa SS, et al. A conceptual model for the coronavirus disease 2019 (COVID-19) outbreak in Wuhan, China with individual reaction and governmental action. Int J Infect Dis 2020;93:211–16.
[15] Shaikh AS, Shaikh IN, Nisar KS. A mathematical model of COVID-19 using fractional derivative. Outbreak in India with dynamics of transmission and control. Preprints 2020.
[16] Khan MA, Atangana A. Modeling the dynamics of novel coronavirus (2019-NCOV) with fractional derivative. Alexandria Eng J 2020. doi:10.1016/j.aej.2020.02.033.
[17] Chanprasopchai P, Ming T ang I, Pongsumpun P. SIR model for dengue disease with effect of dengue vaccination. Comput Math Methods Med 2018;2018:14. Article ID 9861572,
[18] Shah K, et al. Semi-analytical study of pine wilt disease model with convex rate under Caputo-Fabrizio fractional order derivative. Chaos Soliton Fract 2020;135:109754.
[19] Zeigler BP, Kim TGo, Herbert Pr. Theory of modeling and simulation. Academic press 2000.
[20] Rappaz J, Touzani R. On a two-dimensional magnetohydrodynamic problem: modelling and analysis. ESAIM Math Model Numer Anal 1992;26(2):347–64.
[21] Khalid M, Sultana M, Sami F. Numerical solution of SIR model of dengue fever. IntJ Computer Appl 2015;118(21):1–10.
[22] Atangana A, Araz SI. New numerical method for ordinary differential equations: Newton polynomial. J Comput Appl Math 2020;372:112622.
[23] Veeresha P, Prakasha DG, Malagi NS, Baskonus HM, Gao W. New dynamical behaviour of the coronavirus (COVID-19) infection system with nonlocal operator from reservoirs to people. Res Square 2020. doi:10.21203/rs.3.rs-19500/v1.
[24] Anwarud D., Yongjin L., Shah K.. The existence and analytical study of fractional order dynamics of COVID-19 under Attangana-Baleanu-Caputo derivative. To appear (2020);.
[25] Zhou Y. Basic theory of fractional differential equations. Singapore: World Scientific; 2014.
[26] Ulam SM. Problems in modern mathematics. New York: Wiley; 1940.
[27] Ulam SM. A collection of mathematical problems. Interscience, New York 1968.
[28] Ali Z, Kumam P, Shah K, Zada A. Investigation of Ulam stability results of a coupled system of nonlinear implicit fractional differential equations. Mathematics, 2019;7(4):341.
[29] Ali Z, Zada A, Shah K. On Ulam's stability for a coupled systems of nonlinear implicit fractional differential equations. Bull Malays Math Sci Soc 2019;42(5):2681–99.
[30] Ali Z, Zada A, Shah K. Ulam stability to a toppled systems of nonlinear implicit fractional order boundary value problem. Bound Value Probl 2018;2018(1):1–16.
[31] Aphithana A, Ntouyas SK, Tariboon J. Existence and Ulam–Hyers stability for Caputo conformable differential equations with four-point integral conditions. Adv Difference Equ 2019;2019(1):139.
[32] Sonal J. Numerical analysis for the fractional diffusion and fractional buckmaster equation by the two-step laplace Adam-Bashforth method. Eur Phys J Plus 2018;133(1):19.
[33] Sohail A, Maqbool K, Ellahi R. Stability analysis for fractional-order partial differential equations by means of space spectral time Adams-Bashforth moulton method. Numer Methods Partial Differ Equ 2018;34(1):19–29.
[34] Hahm N, Hong BI. A generalization of the Adam-Bashforth method. Honam Mathematical J 2010;32:481–91.
[35] Mekkaoui T, Atangana A. New numerical approximation of fractional derivative with non-local and non-singular kernel: application to chaotic models. Eur Phys J Plus 2017;132(10):444.
[36] Abdon A, F G-AJ. Numerical approximation of Riemann-Liouville definition of fractional derivative: from Riemann-Liouville to Atangana-Baleanu. Numer Methods Partial Differ Equ 2018;34(5):1502–23.